2.0 REVIEW OF PREVIOUS WORK

2.1 Introduction

Since 1984, there have been an increasing number of case studies where aging effects in sands were observed. Most of the data from field studies come from quality control programs, which were used to evaluate the effectiveness of ground modification at a site. Unfortunately, variables that may be potentially relevant to aging effects such as sand mineralogy, temperature, pore fluid composition, and variability of the soil properties are not usually recorded. Therefore, it is difficult to draw conclusions from individual studies and a review of the general body of case studies is needed.

A review of examples of aging effects in sands from the literature is presented in this chapter. The examples are grouped according to the property affected, and include small strain shear modulus, electrical and thermal conductivity, liquefaction resistance, stiffness and shear strength, and the penetration resistance of the sand. This review of examples of observed aging effects in sands draws heavily on a prior study by Human (1992).

2.2 Aging Effects on the Small Strain Shear Modulus of Sands

The small strain shear modulus, G_o, is an important parameter for many geotechnical analyses in earthquake engineering and soil dynamics. The value of G_o depends on a number of parameters, including void ratio, confining stress, soil structure, degree of saturation, temperature, stress history, and time. Afifi and Woods (1971) performed resonant column tests on samples of air-dried medium sand, silt, and kaolinite clay to measure G_o. A constant confining pressure was applied for up to 70 days, and results showed that the small strain shear modulus increased linearly with the logarithm of time. This is shown for Ottawa sand in Figure 2.1. This increase with time can be expressed by the equation

$$G_o(t) = G_o(t_o)\left[1 + \left(N_G \log\left(\frac{t}{t_o}\right)\right)\right] \quad (2.1)$$

where

$G_o(t)$ = Small strain shear modulus at some time t

$G_o(t_o)$ = Small strain shear modulus at an initial time t_o, usually taken at 1000 minutes

N_G = Slope of the relationship between the small strain shear modulus, normalized with respect to $G_o(t_o)$, and logarithm of time

Values of N_G ranged from 2-5% for the air-dried sands to 5-12% for the air-dried silts and clays. Afifi and Woods concluded from these results that the rate of increase in the small strain shear modulus with time increased with decreasing particle size of the soil. In similar studies, Afifi and Richart (1973) and Anderson and Stokoe (1978) reported N_G values for dry sand specimens of <3% and 1%, respectively.

Also shown in Figure 2.1 is the measured vertical strain during the test. In all of these cases, there was very little change in the void ratio of the samples, and the measured increases in small strain shear modulus could not be explained by an increase in density.

Jamiolkowski (1996) reported the values of N_G for several sands, as shown in Table 2.1. Note that sands with significant amounts of carbonate minerals show higher values of N_G than do silica sands.

The time-dependent increase in the small strain shear modulus is very sensitive to disturbance (Thomann 1990; Thomann and Hryciw 1990). A dynamic disturbance, which could result from such things as earthquake loading, blast densification, and vibrocompaction, can partially or completely destroy any previous time-dependent increase in the modulus. Thomann investigated the factors influencing the magnitude and duration of disturbance by measuring the development of the small strain shear modulus during resonant column tests. The magnitude of shear strain was found to be the governing factor in

the magnitude of the modulus decrease. For shear strains less than 0.1%, the decrease in modulus was temporary. For shear strains larger than 0.1%, the small strain shear modulus did not return to pre-disturbance values. However, the specimens were only aged for three days following the shear deformations. This may have been too short a time to regain the pre-disturbance values.

Table 2.1 Values of N_G for various soils (after Jamiolkowski 1996).

Soil	N_G (%)	Notes
Ticino sand	1.2	Predominantly silica
Hokksund sand	1.1	Predominantly silica
Messina sand and gravel	2.2-3.5	Predominantly silica
Messina sandy gravel	2.2-3.5	Predominantly silica
Glauconite sand	3.9	50% Quartz 50% Glauconite
Quiou sand	5.3	Carbonatic
Kenya sand	12	Carbonatic

Human (1992) performed a study on the effects of time on the shear wave velocity of dry sand in triaxial tests using piezoceramic bender elements. Using bender elements for the measurement of shear wave velocity is discussed in detail in chapter four. The shear wave velocity can be related to the small strain shear modulus using the theory of elasticity, and can be written as

$$G_o = \rho v_s^2 \qquad (2.2)$$

where

G_o = small strain shear modulus

ρ = mass, or total, density

v_s = shear wave velocity

The effects of confining stress, density, stress anisotropy, and saturation on the rate of velocity increase with time were measured. The term V_α, defined as the slope of the

shear wave velocity – logarithm time relationship, was used to assess the aging effects. V_α is analogous to the term N_G mentioned above.

For effective confining stresses of 50 to 300 kPa, there appeared to be no trend in how the confining stress affected V_α. There was, however, an increase in V_α as the relative density decreased from 78% to 48%. Samples were tested at different ratios of σ'_3/σ'_1 (1, 0.7, 0.4), and as the degree of anisotropy increased, the value of V_α decreased. The two samples that were saturated prior to aging showed no increase in the shear wave velocity with time.

2.3 Aging Effects on the Thermal and Electrical Conductivity of Sands

In soil mechanics, conductivity refers to the ease with which something can pass through soils and rocks (Mitchell 1993). The most common example is the flow of water through soils, which is characterized by the hydraulic conductivity. Similarly, thermal conductivity can be used to quantify the heat transfer through a soil and the electrical conductivity for the flow of electricity through soil.

Thermal and electrical conductivity measurements in soils are relatively easy to make, and they are thought to be non-destructive (i.e. they do not alter the properties of the specimen being tested). Because of this, and because conductivity can be related to the compositional and structural characteristics of a soil, conductivity measurements have been used to observe aging effects in sands in the laboratory. Brandon and Mitchell (1989) measured the thermal resistivity, which is the inverse of the conductivity, with time for three sands: Monterey No. 60, Surge sand, and Crystal silica sand. The results, shown in Figure 2.2, show that the thermal resistivity for the Crystal silica sand decreased by approximately 20% over a period of 60 days before becoming constant. On the other hand, the thermal resistivity of both the Monterey No. 60 and the Surge sand remained constant over the same period of time. Scanning electron micrographs were reported to show evidence of material accumulation between the grains of the Crystal silica sand. It

was postulated that there was formation of silica-acid gel at the grain contacts, and that this accounted for the decreased resistivity.

Human (1992) studied aging effects in Crystal silica sand by measuring the electrical conductivity. During this study, it was discovered that Crystal silica sand contains approximately 1% montmorillinite. Accordingly, it is possible that material that had accumulated between sand grains in Brandon's experiment was clay. The presence of clay particles, which are negatively charged, confuses the results of electrical conductivity measurements because of surface conductance effects of the particles. In effect, the diffuse ionic double layer surrounding the clay particles provides an additional path for current flow. Human was able to measure time-dependent property changes with electrical conductivity measurements, however, the presence of the clay made interpretation of the results difficult.

2.4 Aging Effects on Liquefaction Resistance

Seed (1979) recognized the significance of time on the liquefaction resistance of sand deposits. He presented results of a laboratory testing program in which cyclic triaxial tests were performed on Monterey No. 0 sand. Samples were prepared to a relative density of 50% and consolidated for different periods of time under an effective confining stress of 155 kPa. The consolidation times were 0.1, 1, 10, and 100 days. A clear aging effect was observed; there was a 12% increase in liquefaction resistance at 10 days and a 25% increase after 100 days of aging. This data was compared to the results of tests on undisturbed specimens, as shown in Figure 2.3. From this, Seed concluded that the liquefaction resistance of natural deposits might be as high as 75% greater than that of freshly deposited laboratory specimens. He also postulated that some form of cementation or cold welding was responsible for the aging effect, but no evidence of this was presented.

Ishihara (1985) also presented examples of the effect of aging on liquefaction resistance. Instead of aging specimens in the laboratory, however, Ishihara compared undisturbed

and reconstituted specimens of Niigata sand. The undisturbed specimens were obtained using a large diameter sampler, and the results of the tests are shown in Figure 2.4. It was found that the cyclic shear resistance was consistently higher for the undisturbed specimens than for the reconstituted specimens. The difference between the two was more pronounced for samples subjected to a higher cyclic stress ratio, which then failed in a fewer number of cycles of loading.

More recently, Arango and Migues (1996) investigated the performance of sand deposits older than 10,000 years within the area affected by the Northridge earthquake in January 1994. A search was undertaken to find sites of older sand deposits near sites that had liquefied. The Tapo Canyon sand met the search criteria and 18 cyclic triaxial tests were performed on both undisturbed and reconstituted samples. Figure 2.5 shows a typical pore pressure response due to cycles of loading for an undisturbed (cut from a block sample) and reconstituted sample. The pore pressure ratio, r(u), is defined as the change in pore pressure divided by the effective confining stress. The results showed that the development of pore pressure was much less in the undisturbed sample, corresponding to an undisturbed cyclic strength that was significantly higher than the reconstituted cyclic strength.

In order to investigate the hypothesis that cementation at the particle contacts was responsible for the increased strength, Arango and Migues (1996) performed controlled freezing and thawing of the undisturbed samples. This was done to impose small but uniform volumetric strains that might break any brittle bonds without altering the fabric of the samples. The results showed that the pore pressure response under cyclic loading was not changed significantly by the freeze/thaw process, and it was postulated that increased interlocking caused by infilling or overgrowth was responsible for the aging effects.

The undisturbed cyclic strength of the Tapo Canyon sand was also compared to the cyclic strength that would correspond to a “young” (<10,000 years) sand deposit. From the

measured blow counts at the site, a cyclic stress ratio corresponding to liquefaction was estimated using the empirical chart developed by Seed et al. (1984). The chart was developed from field data of "young" deposits, and did not reflect the behavior of sand deposits greater than 10,000 years old. The measured cyclic strength of the Tapo Canyon sand was 1.6 to 2.7 times greater than the estimated cyclic strength using the empirical approach. This data, along with data obtained in a similar manner from two sites in South Carolina, is shown in Figure 2.6.

2.5 Aging Effects on the Stiffness and Shear Strength of Sands

Some of the earliest work on the time-dependent properties of sands was performed in the former Soviet Union. Denisov and Reltov (1961) studied the development of adhesion between sand grains and a quartz plate with time. An experimental program was developed which involved placing the grains on a vibrating quartz or glass plate and measuring the shear force necessary to move the grains. The equipment setup used in the experiments is shown in Figure 2.7. The dry grains were allowed to sit on the plate for varying times (up to 20 hours), after which the sand and plate were submerged in water and vibrated. The amount of time that the sand was submerged before vibration occurred was also varied (42 hours, 6 days, and 14 days).

Figure 2.8 shows the results of the vibrating plate experiments. The ordinate is the shear force required to move the sand grain normalized with the shear force measured after 20 hours of dry contact. The abscissa is the time of dry contact before the sand was submerged, and each line represents different periods of soaking. These results show that the shear force required to move the sand grains increased as the amount of time the plate was submerged increased. In fact, there was an approximately 320% increase in the measured shear force between the grains that were submerged for 14 days after 20 hours of dry contact and the grains that had only had a 20 hour period of dry contact.

Denisov and Reltov hypothesized that the increase in shear force with time was caused by the formation of a thin layer of silicic acid gel around the sand grains, resulting from dissolution of the sand by the water. However, there was no explanation of the increase in shear force during the 20 hours of dry contact only.

As a part of a larger study on the influence of stress history on the stress-strain behavior of sand, Daramola (1980) investigated the effects of aging on both the stiffness and shear strength. Four consolidated drained tests on Ham River sand were performed. Each sample was prepared to the same density but consolidated for different periods of time (0, 10, 30 and 152 days). The effective confining stress was 400 kPa throughout the tests. The results, shown in Figure 2.9, show that the stiffness increased and the strain to failure decreased with increasing time of consolidation. The volumetric strain data also shows that the axial strain at which the soil became dilatant decreased with increasing time. From the results, the author concluded that a 50% increase in modulus occurs for each log cycle of time. Despite the increase in modulus and dilatancy, however, there was no increase in the shear strength of the sand with time.

Schmertmann (1991) postulated that the aging process for both clays and sands was entirely frictional in nature, resulting from some combination of dispersive particle movements, internal stress arching, and increased interlocking. Evidence presented to support this hypothesis relied heavily on the results of IDS tests, which were developed (Schmertmann 1976; 1981) to separate the frictional and cohesive components of shear strength. Details of this evidence are presented in section 3.2.

Schmertmann also presented the results of a new test in which a quasi-preconsolidation pressure was measured for the first time in a sand specimen. This term was first used by Leonards and Ramiah (1959) to describe the reduction in stiffness and increase in preconsolidation pressure that occurs during periods of secondary compression in normally consolidated clays. An 8-inch diameter plate load test was performed in a large box

containing dry quartz sand. The load on the plate was incrementally increased and the corresponding settlements were measured. One of the loads was kept on the sand for 844 minutes before the next load was applied. Figure 2.10 shows that, after 844 minutes, the stiffness of the sand to loading increased significantly, and this effect continued until a quasi-preconsolidation pressure of 350 pounds was exceeded. Prior to performing the load test, however, the sand was first loaded laterally to passive failure for a few minutes and then unloaded to active horizontal stress conditions for approximately 30 minutes. This was accomplished with lateral air bags mounted on the sides of the box. It is not clear how the above loading cycles affected the soil, but without it Schmertmann was unable to produce the quasi-preconsolidation effect.

Human (1992) conducted three consolidated drained triaxial tests in a study similar to that of Daramola (1980). These tests were part of a larger study to determine the effect of time on the shear wave velocity of sand as described in section 2.2. Dry Crystal silica sand was used for the tests, and the samples were prepared to a relative density of 78%. Each sample was consolidated for different periods of time (1 hour, 3 days, 28 days), and the results of the tests are shown in Figure 2.11. Shear wave velocity measurements were made throughout each test and Figure 2.11 (a) shows a consistent increase in the shear wave velocity, and thus in the small strain shear modulus, with time. Despite this, however, there was very little difference between the modulus during shear and strength of the three samples, as shown in Figure 2.11 (b).

Pender et al. (1992) reported the results of cyclic simple shear tests done on different types of pavement base course materials to measure changes in the density and stiffness under repeated loading. Strain controlled tests were performed with up to 500,000 cycles of deformation. These tests were conducted over a five-day period, with 100,000 cycles per day. After each day, the specimens were rested overnight before the next stage of cycles resumed. At the resumption of testing each morning, the measured secant shear modulus was found to have increased 10 to 17%, as shown in Figure 2.12 (a). It was also

found that the magnitude of the increase was larger for tests run at smaller strain levels. Figure 2.12 (b) shows that there was no corresponding increase in density during the time between loadings to account for the measured increase in secant modulus. The ordinate in Figure 2.11 (b) is the current density divided by the initial density.

Most recently, Martin et al. (1996) found that time-dependent changes in stiffness can be caused by bacterial growth. A study was conducted on the feasibility of using bacteria and biopolymers for the construction of impervious barriers. Triaxial tests were performed on samples with up to 45 days of aging. Results of the laboratory tests showed that bacteria and biopolymer (Xanthan gum) laden pore water reduced the hydraulic conductivity of a silty soil by 100 times and increased the shear strength by 50%. Results of the strength testing are shown in Figure 2.13. The dashed line in Figure 2.13 shows the baseline strength of the soil without bacteria or biopolymers. However, it is not clear if the "clean" specimens were actually aged or whether the curve was extrapolated from the strength of the fresh specimens.

2.6 Aging Effects on the Penetration Resistance of Sands

Most of the examples of aging effects in the literature involve in situ tests such as the cone penetration test. Fifteen separate case studies are presented and discussed below.

2.6.1 Jebba Dam Project (Mitchell and Solymar 1984)

The Jebba Dam project was the first well-documented field case where aging effects were both significant and widespread. The project involved the improvement of the foundation soils beneath a proposed 42 m high dam and seepage blanket on the Niger river in Nigeria. The foundation soils consisted of deep deposits of alluvial sand, the properties of which are summarized in Table 2.2. In some areas the depth to bedrock was greater than 70 m. Due to the variable relative density of the deposit, the large loads associated with the dam, and the potential for liquefaction during an earthquake, differential settle-

ments that would cause cracking of both the dam core and the seepage blanket were a major concern.

Table 2.2 Properties of Jebba Sand.

Sand Description	Subrounded to rounded coarse silica sand 91.8% quartz, 2.2% granites, 2% volcanics, 1.6% feldspar, 1.4% gneiss, 1% chert
Uniformity Coefficient, C_u	2.94
Average Saturated Unit Weight*	20.1 kN/m^3
D_{50}	0.17 – 4.30 mm

* Ranged from 19.3 kN/m^3 to 21.1 kN/m^3

A two stage densification program was designed to deal with the large depths of the loose zones in the sand deposit. The upper 25 m of sand (and a 5 to 10 m thick sand pad placed by hydraulic filling of the river) was densified using vibrocompaction. Blast densification was used to densify the deeper loose zones between 25 and 40 m depth.

During blasting, it was observed that the sand exhibited both sensitivity (i.e. strength loss on disturbance) and aging effects. A typical example of the initial decrease in penetration resistance after blasting densification and subsequent increase with time is shown in Figure 2.14. This phenomenon occurred throughout the site and followed a general pattern. Initially after improvement, there would be a decrease in penetration resistance despite the fact that surface settlements ranging from 0.3 m - 1.1 m were measured, which would imply an increase in density. With time (measured up to 124 days after improvement), however, the cone penetration resistance was found to increase by approximately 50-100% of the original values.

Aging effects were also observed after both placement of hydraulic fill and vibrocompaction. In the case of vibrocompaction, however, there was considerable variability in the magnitude of the aging effects throughout the site. It is interesting to note that, unlike

the areas where blast densification was performed, the penetration resistance immediately after vibrocompaction was always higher than before compaction. Examples of the increase in penetration resistance with time after vibrocompaction and placement of hydraulic fill are shown in Figures 2.15 and 2.16, respectively.

Mitchell and Solymar discussed a number of possible mechanisms that could have been responsible for the phenomenon. Time-dependent strength gain due to pore pressure dissipation was discounted because complete dissipation occurred in the order of hours, whereas, the aging effects were measured over a period of days and months. Thixotropy was also discounted as a possible mechanism because it is thought to be caused by small net differences in attractive/repulsive forces in fine-grained soils (Mitchell 1993), which are not relevant in sands. Mitchell and Solymar believed that the mechanism most likely responsible for the aging effects was formation of silica acid gel films on the surface of particles. It was suggested that these films could develop with time to act as a cementing agent between sand grains, however, no direct evidence was presented to support this hypothesis.

2.6.2 Laboratory Study of Blast Densification (Dowding and Hryciw 1986)

Mini-cone penetration tests were used to assess the effectiveness of blast densification of saturated sand under controlled conditions in the laboratory. As part of the study, the effects of aging on penetration resistance were also investigated. A large (1 m diameter, 1 m high) circular liquefaction tank was used for all the tests, and a local beach sand from the campus of Northwestern University was used for all the tests. The properties of the Evanston sand are shown in Table 2.3.

The sand was prepared to an initial relative density of 50% for all tests. The height of the samples in the tank was approximately 66 cm. The testing program was set up so that, following a blast that was set off in the center of the tank, penetration tests could be performed at different radial distances (10, 20, 30, and 40 cm) and at different times (pre-

blast, 1 day, 5 days, and 15 days). After blasting, the relative density ranged from 63% to 78%. Time-dependent increases in penetration resistance were found in both a control test, in which no blasting was done, as well as in the tests with blasting. The results from these tests are shown in Figure 2.17. These results are plotted as the change in penetration resistance from pre-blast values as a function of time and radial distance from the point of detonation. It can be clearly seen that the penetration resistance increased with time for all cases, and that the aging effects were larger for the tests involving blasting. In addition, the greatest increases were consistently found to occur near the blast location. It is also apparent, however, that near the center of the blast, the 1 day readings either decreased or were unchanged compared to the no blast readings. This may be the result of a cavity that was created by the blast or blast gases, rather than the "sensitivity" discussed in the previous example. Dowding and Hryciw postulated that the increase in penetration resistance with time could be caused by the gradual dissipation of the blast gases, which may have created an arching effect in the soil.

Table 2.3 Properties of Evanston Beach Sand.

Description	Fine, poorly graded, brown, silica sand
Coefficient of Uniformity, C_u	1.5
Specific Gravity, G_s	2.67
Minimum Dry Unit Weight, γ_{min}	14.5 kN/m^3
Maximum Dry Unit Weight, γ_{max}	16.5 kN/m^3
D_{50}	0.2 mm

2.6.3 Field Study of Blast Densification (Hryciw 1986)

In conjunction with the laboratory study described above, Hryciw (1986) performed a field test to assess the effectiveness of blast densification of a saturated sand deposit. The site of the experiment was in southeastern Georgia, and consisted of 3 to 9 m of loose saturated sand overlain by 1.5 – 2 m of stiff clay and vegetation. The sand was very fine (D_{50} = 0.10 to 0.15 mm) and was poorly graded with 5 to 15% silt. Blasting was performed in a single hole at a depth of 7 m and cone penetration tests were performed at various radii (0.9, 3.0, 5.5, 7.6, and 12.2 m) away from the blast. A series of these tests

was performed prior to blasting, 1 to 2 days after, and 30 days after blasting to study any change in penetration resistance with time.

Following blasting, there was an immediate decrease in the penetration resistance. This decrease occurred despite the observation of surface settlement radially about the blast hole. During these cone penetration tests, water was reported to have flowed out of the boreholes as the stiff clay layer was penetrated. This made it difficult to determine if the decrease was due to sensitivity of the deposit or due to excess pore pressures. After 30 days, however, there was still no change in the values of cone penetration resistance from the 1 to 2 day tests.

2.6.4 St. Johns River Power Park (Schmertmann et al. 1986; Schmertmann 1987)

Schmertmann et al. (1986) reported on a case study in which the foundation soils for a large power plant near Jacksonville, Florida were improved using both dynamic compaction and compaction grouting. The quality control program was extensive and involved 908 cone penetration tests and 33 flat plate dilatometer tests (DMT).

The site was located in a naturally filled-in former marine estuary. The upper 10 m consisted of an uncemented loose, relatively clean quartz sand. From approximately 10 to 17 m depth the clean quartz sand was interspersed with fine layers of silt and clay.

The effects of aging were studied on a test section at the site where there had been densification by dynamic compaction. The results of these tests are shown in Figure 2.18. The increase in penetration resistance with time was correlated to the number of drops used for the dynamic compaction and the depth within the soil profile. From this figure, time improvement factors for cone penetration resistance were developed and were used to adjust measured post-densification penetration resistance values to specific times after compaction. These improvement factors are listed in Table 2.4.

Table 2.4 Time Improvement Factors for q_c at Power Plant Site.

Time Between DC and CPT (days)	Factor by Which to Multiply q_c
5	1.35
10	1.20
15	1.15
20	1.12
30	1.06
40	1.03
50	1.01
60	1.00

Two things are worth noting in Figure 2.18. First, the results suggest that the amount of energy input by the dynamic compaction process not only affects immediate improvement but also affects the subsequent time-dependent increase in penetration resistance. This is indicated by the fact that the aging effect increased as the number of drops increased. Second, there is significant scatter in the data, and the trend lines chosen by Schmertmann are very subjective.

2.6.5 Pointe Noire Deep Sea Harbor (Dumas and Beaton 1988)

In Sept-Iles, Quebec, dynamic compaction was performed as part of a deep sea harbor project. The densified deposit was 6 to 17 m thick and was hydraulically placed by end dumping from the surface. The hydraulic fill was a medium to coarse grained sand with an average grain size of 0.79 mm and a uniformity coefficient of 3.06.

It was reported that, in some locations, there was a 100% increase in cone penetration resistance between tests performed immediately after compaction and subsequent tests performed 18 days later. Figure 2.19 shows cone penetration test results at one area at three different times: immediately after placement of hydraulic fill, immediately after dynamic compaction, and 8 days after the first pass of dynamic compaction.

The authors compared these results with the Jebba Dam case study. The increase in penetration resistance occurred much more quickly than at Jebba and no sensitivity of the sand deposit was observed. The lack of sensitivity was attributed to the fact that the fill was freshly deposited, and thus did not have time to develop any structure. It is also possible that, like vibrocompaction, the densification from dynamic compaction could have been large enough to overcome any initial strength loss caused by sensitivity. It was also suggested that the aging effects were related to the energy input during densification, because as shown in Figure 2.19, the increase in penetration resistance with time was greater near the surface and diminished with depth. This trend is qualitatively similar to how energy from the dynamic compaction process attenuates with depth.

2.6.6 Tarsiut P-45 Caisson, Beaufort Sea (Jefferies et al. 1988)

Jefferies et al. (1988) present a brief study of aging effects during the construction of an artificial island in the Beaufort Sea. The island was actually a large mobile caisson, called Molikpaq, used for offshore oil drilling in the Arctic. To form the island, designated Tarsiut P-45, approximately 20 m of sand fill was placed hydraulically through seawater. The sand used was called Erksak fill, with a D_{50} of 0.3-0.4 mm and <8% silt. As placed, the relative density of the fill was approximately 60%. The average temperature of the sand was ~0^{o} C. Penetration tests were performed six days and eleven months after placement to assess any aging effects. The eleven month penetration tests were performed within 1.5 m of the location of the six day tests. There was no measured increase in the penetration resistance with time.

2.6.7 Amauligak F-24 Caisson, Beaufort Sea (Rogers et al. 1990; Jefferies and Rogers 1993)

Another mobile Arctic caisson, Amauligak F-24, was hydraulically filled with the same sand described above. However, in this case, blast densification was used to increase the density of the fill. Cone penetration test results from before and at two times after blasting are shown in Figure 2.20. It was reported that there was a substantial increase in the

penetration resistance after two to five days, and there was continued improvement for several weeks. No sensitivity of the deposit was observed.

2.6.8 Field Study of Blast Densification (Thomann 1990)

Thomann (1990) performed a field study on the effect of blast densification on both the cone penetration resistance and the shear wave velocity with time. This field study was done in conjunction with the laboratory testing program on the effect of disturbance on the small strain shear modulus discussed in section 2.2. The tests were performed at Douglas Lake in Cheboygan county, Michigan in a partially saturated, medium dense sand deposit. The properties of Douglas Lake sand are shown in Table 2.5.

Table 2.5 Properties of Douglas Lake sand.

Sand Description	Poorly graded, fine to medium, subangular sand
Uniformity Coefficient, C_u	2.42
D_{50}	0.25 mm
Minimum void ratio, e_{min}	0.54
Maximum void ratio, e_{max}	0.82

Penetration tests and shear wave velocity measurements were performed with a seismic cone before and at four times following blasting (1, 3, 4, and 217 days). There were no measured increases in either the cone penetration resistance or the shear wave velocity with time. In fact, both the cone penetration resistance and the shear wave velocity decreased immediately following blasting and never reached the pre-blast values. Thomann postulated that the property decreases may have resulted because the sand was initially dense and that the blasting actually caused some loosening of the deposit.

2.6.9 Compaction of a Deep Hydraulic Fill (Massarch and Heppel 1991)

An example of aging effects was presented as part of a report on the use of the Müller Resonance Compaction system (MRC), a type of vibratory probe for deep vibratory compaction. A 26 m layer of hydraulic fill, consisting of a very loose to loose sand inter-

spersed with layers of clay and silt, was compacted using the MRC system at a site in Hong Kong. The groundwater table at the site was located approximately 3 m below ground surface. Penetration tests were performed some time (not stated) after compaction and also 1 year after compaction. It was reported that after 1 year the penetration resistance had increased 50% since the first readings. The data presented, however, contained considerable scatter, which was attributed to the interspersed silt and clay layers.

2.6.10 Cone Penetration Testing Following the Loma Prieta Earthquake (Human 1992)

The magnitude 7.1 Loma Prieta earthquake, which struck the San Francisco, CA area on October 17, 1989, caused widespread liquefaction at Bay Farm island in Alameda. Bay Farm Island is a man-made island formed by hydraulic filling in the 1960's. Because there were cone penetration records from before the earthquake, Human (1992) performed additional penetration tests with time after the earthquake to assess the effect of the earthquake on the soil properties at the site. Tests were performed 4, 14, 30, 65, and 317 days after the earthquake. For each time, four penetration tests were performed to assess the variability of the readings.

The site consisted of 4 m hydraulically placed fine silty sand underlain by a soft clay layer of variable thickness (also fill). Beneath the fill was 3 m of soft to medium stiff clay (Bay Mud) and Holocene sands. The groundwater table was 2 m below the ground surface.

Four days after the earthquake, there was no change in the penetration resistance from the pre-earthquake values, despite the presence of sand boils on the site. Over the 317 days, there was some increases in the penetration resistance, however, it was not consistent with depth. Furthermore, the variability at each was assessed from the four cone penetration tests. It was determined that the observed increases were within the natural variability of the deposit, which made interpretation of the aging effects very difficult. Most

of the examples in this chapter present only one cone penetration test at each time, and this case study point out how important it is to assess the natural variability of a site.

2.6.11 Field Blasting Experiment in Greeley, Colorado (Charlie et al. 1992)

An investigation of the effects of blasting and time on the three components of the cone penetration test (tip resistance, skin friction, and friction ratio) was undertaken by Charlie et al. (1992). Blast densification was performed in Greeley, Colorado between November and March of 1987. The site consisted of 1.5 m of a poorly graded medium to fine sand overlying 3.6 m of a poorly graded gravelly sand. Beneath the gravelly sand was a layer of inorganic silt. The properties of the two sands are shown in Table 2.6. The relative densities of the sands classified them as dense to very dense deposits.

Table 2.6 Properties of Sand from Greeley, Colorado.

Description	Poorly graded medium to fine sand (SP)	Poorly graded gravelly sand (SP)
Coefficient of Uniformity, C_u	4.9-5.6	4.17-5.75
D_{50}	0.80-1.80 mm	2.1-2.3 mm
D_{10}	0.19-0.30 mm	0.51-0.62 mm
Specific Gravity, G_s	2.62	2.62
Petrographic Analysis	80% quartz; 10% igneous and metamorphic; 5% feldspar	80% quartz; 10% igneous and metamorphic; 5% feldspar
Minimum Dry Unit Weight $\gamma_{d\ min}$	-	16.5-16.6 kN/m^3
Maximum Dry Unit Weight $\gamma_{d\ max}$	-	18.8-19.4 kN/m^3
Relative Density, D_r	70-90%	70-85%

Cone penetration tests were performed before and at several times after blasting. One week after blasting, both the tip resistance and sleeve friction were less than pre-blast values. Additional penetration testing was then performed 3 weeks, 18 weeks, and 5 1/2 years (Charlie et al. 1993) after blasting. After 18 weeks, the normalized tip resistance was found to have increased 18%, while the sleeve friction was found to have decreased 39% with respect to the 1 week values. After 5 1/2 years, the tip resistance had increased

211% and the sleeve friction had decreased 42%, again with respect to the 1 week values. Only the 5 1/2 year penetration resistance was greater than the pre-blast values, which was attributed to the initial high relative density of the sands. The sleeve friction continued to decrease from 1 to 18 weeks, and this led the authors to conclude that the horizontal stresses were decreasing with time.

Charlie et al. (1992) also compiled data on the increase in penetration resistance following ground improvement from a number of other cases found in the literature. The results of the compilation were plotted in the form of normalized penetration vs. time, as shown in Figure 2.21. Based on this data, the following empirical equation was presented:

$$\frac{(q_c)_{N\ weeks}}{(q_c)_{1\ week}} = 1 + K \log N \qquad (2.3)$$

where

q_c = tip resistance

N = number of weeks since improvement

K = the slope of the penetration resistance – log time relationship

The values for the empirical constant, K, as determined from Figure 2.21, are listed in Table 2.7.

Table 2.7 Empirical Constants for Aging Effects in Penetration Resistance (Charlie et al. 1992).

Reference	Type of Densification	K
Mitchell and Solymar (1984)	vibrocompaction	1
Mitchell and Solymar (1984)	blast densification	0.7
Schmertmann et al. (1986)	dynamic compaction	0.3
Charlie et al. (1992)	blast densification	0.13
Jefferies et al. (1988)	hydraulic fill	0.02

The rate of increase of aging effects (quantified by K) was then correlated to the assumed air temperatures of the published case histories, as shown in Figure 2.22. The results showed K was larger at sites in warm climates than at sites in colder climates. Based on

this, the authors concluded that the aging process was temperature dependent and that cementation may be the mechanism responsible.

However, in a discussion of this study, Jefferies and Rogers (1993) disagreed with the temperature data that was used by Charlie et al. to suggest that the aging process was temperature dependent. Specifically, they asserted that actual ground temperature rather than mean air temperature data should be used. Figures 2.20 and 2.21 are the revised plots using the actual ground temperature data from Jefferies et al. (1988) and Rogers et al. (1990). With the revised results the effect of temperature on the increase in the penetration resistance was shown to be much smaller than originally indicated.

2.6.12 Field Blasting Experiment in Kelowna, B. C. (Gohl et al. 1994)

In order to gain experience with blast densification, Gohl et al. (1994) performed blasting at a test site in Kelowna, British Columbia. The site consisted of approximately 2 to 3 m of random fill overlying loose sands. Blasting caused liquefaction of the sand layer, which was apparent by large amounts of water that bubbled to the surface and by measured settlements of up to 1 m. Two passes of blasting were performed and cone penetration tests were performed up to 450 days after blasting. A time-dependent increase in penetration resistance was measured in some locations. However, it was reported that the increase was not consistent throughout the site. It was not reported whether the site exhibited any sensitivity immediately after blasting.

2.6.13 Blast Densification at the SM-3 site (AGRA 1995; Ground Engineering 1995)

A large blast densification project in the Saint Marguerite River northwest of Sept-Iles, Quebec was performed between February and April of 1995. A 100 m by 120 m area of the river bed was densified in order to reduce the potential for static liquefaction and improve the stability of an excavation for a cofferdam during construction of a main dam. Drilling and blasting were done from a compacted layer of snow and ice, which covered the river up to a thickness of 1.3 m.

The soils at the site consisted of 10 to 20 m of loose sand overlying dense sand, underlain by more loose sand. The properties of the sands found at the site are shown in Table 2.8. The initial relative density of the loose sand was estimated from cone penetration tests to be 40%. The blasting program improved the relative density throughout the site to an average of 60%. In one area of the site, cone penetration testing was performed before and after blasting at intervals of 2, 12, and 35 days. The results, shown in Figure 2.23, indicate that after 2 days there was either no improvement or even a slight decrease in the penetration resistance. Twelve days after blasting, the penetration resistance was found to be 2 to 3 times higher than pre-blast values. After 30 days, however, there was only slight improvement over the 12 day values.

Table 2.8 Properties of Sand from the Saint Marguerite River.

Coefficient of Uniformity, C_u	1.9-4.5
Coefficient of Curvature, C_c	0.9-1.8
D_{50}	0.3-1.5 (0.75 average)
Minimum Dry Unit Weight $\gamma_{d\ min}$	14.4-15.2 kN/m^3
Maximum Dry Unit Weight $\gamma_{d\ max}$	17.6-18.8 kN/m^3

2.6.14 Laboratory Test on the Penetration Resistance of Sand (Joshi et al. 1995)

A laboratory study was performed by Joshi et al. (1995) specifically to study the effect of time on the penetration resistance. The influences of both sand type and pore fluid composition on the magnitude of aging effects were investigated. Two different sands were tested: a local river sand and Beaufort Sea sand. The properties of these sands are listed in Table 2.9. The sands were tested dry and in distilled and seawater.

Table 2.9 Properties of River sand and Beaufort Sea sand.

	River sand	Beaufort Sea sand
Description	More angular, less rounded	Less angular, more rounded, with some flaky particles
Coefficient of Uniformity, C_u	2.39	2.67
D_{50}	0.41 mm	0.34 mm
Minimum Dry Unit Weight $\gamma_{d\ min}$	14.6 kN/m^3	14.3 kN/m^3
Maximum Dry Unit Weight $\gamma_{d\ max}$	16.6 kN/m^3	16.5 kN/m^3

The sand was placed in 36 cm diameter by 37 cm high PVC cells and subjected to a static vertical stress of 100 kPa. Each specimen was prepared by pluviating the sand through either air or water (depending on the test) and vibrating the specimen under the static load until the desired density was achieved. This method of preparation resulted in the following calculated relative densities:

Dry river sand	87%
Saturated river sand	95%
Saturated Beaufort Sea sand	100%

After loading, the specimens were aged for two years, and values of penetration resistance were obtained at various times in each specimen. Penetration tests in each specimen were performed with a series of four, 1 cm diameter penetrometers so that redundant data could be obtained at each time. For each penetration test, the probe was advanced ~2 mm. Aging effects were observed in all cases. A typical plot of load vs. displacement at various times for one of the penetrometers is shown in Figure 2.24 and appears to clearly show an aging effect. The normalized increase in penetration resistance with time

for the same case is shown in Figure 2.25. Based on these results, it was proposed that the increase in penetration resistance with time follows a general form

$$\frac{P_t}{P_1} = a(t)^b \qquad (2.4)$$

where

P_t = penetration resistance at some time, t, in days

P_1 = penetration resistance at 1 day

a, b = curve fitting parameters with the following values:

	a	b
Dry sand	0.9	0.06
Distilled water	0.75	0.15
Seawater	0.7	0.17

Note that increases in penetration resistance were measured in all three cases. Parameters a and b were determined by curve fitting data from each of the tests. These results suggest that the effect of aging was greatest for sand submerged in seawater and least for dry sand. Equation 2.4 would predict that a sand aged for 1 year would have penetration resistance increases of 90%, 80%, and 30% if saturated in seawater, distilled water, or air, respectively.

In addition to the penetration tests, detailed mineralogical studies using X-ray diffraction and electron microscopy showed the presence of precipitates on the grains of the submerged samples after aging. For the samples of River sand submerged in distilled water, the composition of the precipitates was found to calcium and possibly silica. In the case of the samples submerged in seawater, sodium and chlorine were also found as precipitates. Because aging was observed in dry sand, the authors concluded that, for sands in the dry state, aging effects were caused by rearrangement of particles. In the submerged state, it was hypothesized that the aging effects were the result of a combination of rearrangement of particles and precipitation of the soluble fractions of the sand.

2.6.15 Chek Lap Kok Airport, Hong Kong (Ng et al. 1996)

A recent example of aging effects in sands was reported by Ng et al. (1996) during construction of the Chek Lap Kok airport in Hong Kong. Vibrocompaction was performed in specific areas to improve the penetration resistance of hydraulically placed sand fill. Cone penetration testing was performed at one location at different times, up to 47 days after improvement. A clear increase in penetration resistance was observed, as shown in Figure 2.26. As with the other case studies involving vibrocompaction, there was no sensitivity observed, and the time-dependent increase in cone penetration resistance occurred with little corresponding increase in density.

2.7 Trends

Three tables are included at the end of this section that summarize trends in the case studies presented in this chapter. Table 2.10 provides a summary of the examples presented above. Table 2.10 includes the following specific information (when available) about each example:

- Median particle size
- Coefficient of uniformity
- Relative density
- Vertical effective stress range
- Temperature
- Type of densification
- Measured time period
- Amount of improvement

Tables 2.11 and 2.12 highlight the significant findings of each case study. Table 2.11 includes the examples of time-dependent increases of the small strain shear modulus, conductivity, liquefaction resistance, and stiffness and shear strength, whereas Table 2.12 highlights the main points from the examples of aging effects on the cone penetration resistance.

The median grain size, D_{50}, ranged from 0.10-4.30 mm for the examples shown in Table 2.10. In most of the cases, fine to medium sands were the primary sands studied. However, there are three examples (Mitchell and Solymar 1984; Charlie et al. 1992; AGRA 1995) in which large aging effects were measured in coarse sands. The only example in Table 2.10 that measured no aging effects in the field (Jefferies et al. 1998) involved a medium sand. From these examples, it does not appear that any generalizations can be made with regard to the median grain size.

In all the cases the sands were poorly graded, with most of the sands in the examples having coefficient of uniformity (C_u) values less than 3. Although this is a definite trend within the examples presented, this may not be a good indicator of the potential for aging. Aging effects are usually of interest in loose sand deposits, such as with hydraulically placed fills, or deposits that are to be densified by ground improvement. These types of deposits are frequently uniform, because well-graded sands in nature are generally denser and have smaller void ratios due to the wide range of particle sizes.

The relative density, D_r, in the examples ranges from approximately 20% (very loose) to 100% (very dense). Some of the best examples of aging effects (the Jebba Dam project and the laboratory penetration tests performed by Joshi et al. 1995) involved very loose and dense sands, respectively. There appears to be no correlation between D_r and the rate or magnitude of aging effects. The same can be said for the vertical effective stress range. In the various examples, a wide range of stress levels existed (0-400 kPa), all of which are within the normal range of engineering practice.

From the available data, there also does not appear to be a simple relationship between the amount of aging and temperature. For example, there was no aging reported by Jefferies et al. (1988) for the hydraulic fill placed at 0° C. However, a similar fill under the same conditions showed clear increases in penetration resistance following blast densifi-

cation. In the case of the SM-3 site in Quebec (AGRA 1995), also at approximately 0° C, there was a 200-300% increase in penetration resistance within 12 days.

It is very difficult to draw any significant conclusions on the effect of different methods of placement and densification on aging effects,. For the hydraulic fill that was placed at the Jebba Dam project (Mitchell and Solymar 1986), the cone penetration resistance increased between 30% and 100% between the second set of readings (4 to 10 days after placement) and the third set (50 to 80 days after placement). In contrast, the hydraulic fill placed in the Tarsiut P-45 caisson in the Beaufort Sea (Jefferies et al. 1988) showed no increase in penetration resistance after 11 months of aging.

For densification by blasting, again it is difficult to observe definite trends. In seven of the eight examples, a time-dependent increase was observed. However, in two of the cases (Hryciw 1986; Thomann 1990) the aging effects were not enough to offset the initial reduction in penetration immediately after blasting. Both of these involved medium to dense sands, and it is likely that the blasting actually loosened the deposits. The one example where no aging effects were observed following blast densification in loose sands was at a site where the top 1.5 to 2 m consisted of stiff clay and vegetation (Hryciw 1986). There were clearly excess pore pressures 1 to 2 days after blasting, as evidenced by water flowing out of the bore holes. After 30 days, however, there was still no increase in penetration resistance despite observed surface settlements indicating an increase in the average density of the deposit. Finally, one of the case studies (Gohl et al. 1994) reported some increases in penetration resistance following blast densification; however, the effect was not consistent throughout the site.

Sensitivity does appear to be a common occurrence following blast densification in natural sand deposits. There was only one case where no sensitivity was measured in the field, and it involved the densification of a freshly placed hydraulic fill (Rogers et al. 1990). Likewise, in a laboratory blasting experiment in a liquefaction tank, the only re-

duction in penetration resistance was close to the blast hole, where a cavity or blast gases may have caused the effect.

In the cases where either vibrocompaction or dynamic compaction were performed, there did not appear to be any significant sensitivity measured. In all the examples, there was some initial increase in penetration resistance followed by a variable amount of additional time-dependent increase. In all these cases, the variability from site to site and the scatter in the data make it very difficult to make generalizations about the magnitude or rate of sand aging effects.

It is very difficult to make comparisons between the various examples because of the lack of comprehensive information about each site. Aging effects are rarely the primary goal of a field study, and as such, many of the examples are based on one or two cone penetration tests at random times after ground modification. In most cases, little attention is given to potentially significant details, such as pore fluid composition, temperature, sand mineralogy, and spatial variation of soil properties. It would be useful if there were a standard approach to studying aging effects in the field. Standardization would require guidelines on which properties to measure, when to measure them, and location and number of the tests.

Table 2.10 Summary of aging effects in sands reported in the literature.

Reference	D_{50} (mm)	C_u	D_r %	[1]σ_v' (kPa)	T (°C)	Densification	Measured Time Period	Improvement with Time	Notes
Afifi and Woods (1971)	0.44	1.6	92	138, 207	20	-	108 days	N_G increased 2-5%	Ottawa Sand, air dried Laboratory tests
Afifi and Woods (1971)	0.10	1.5	dense	69, 138	20	-	430 days	N_G increased 2-5%	Agsco No. 2, air dried Laboratory tests
Seed (1979)	0.41	1.4	50	155	20[2]	-	100 days	12% increase in liquefaction resistance at 10 days; 25% increase after 100 days	Monterey No. 0 Laboratory tests
Ishihara (1985)	0.30	2.5	40-70	20-120	20[2]	-	-	Undisturbed liquefaction resistance higher than reconstituted samples	Niigata sand, saturated Laboratory tests
Daramola (1980)	NA	NA	66	400	20[2]	-	152 days	50% increase in shear modulus per log cycle of time	Ham River sand, saturated; Laboratory tests
Mitchell and Solymar (1984)	0.44-0.90	2.94 (1.52-8.83)	40-70	0-200	27	Hydraulic fill	50-80 days	30-110% increase in q_c between 4-10 day readings and 50-80 day readings	Alluvial sand; 91.8% quartz, 2.2% granites, 2% volcanics, 1.6% feldspar, 1.4% gneiss, 1% chert
Mitchell and Solymar (1984)	0.33-2.5	2.94 (1.52-8.83)	40-70	100-460	27	Vibrocompaction	24 days	Variable increase in q_c. No sensitivity.	Alluvial sand; 91.8% quartz, 2.2% granites, 2% volcanics, 1.6% feldspar, 1.4% gneiss, 1% chert
Mitchell and Solymar (1984)	0.18-4.3	2.94 (1.52-8.83)	40-70	360-610	27	Blasting	124 days	50-100% increase in q_c Sensitivity immediately after blasting	Alluvial sand; 91.8% quartz, 2.2% granites, 2% volcanics, 1.6% feldspar, 1.4% gneiss, 1% chert
Dowding and Hryciw (1986)	0.20	1.5	50	~0	20[2]	Blasting	15 days	Penetration resistance increased 75-90% in 15 days. Effects also observed w/out blasting. Aging effects greatest near blast. Little sensitivity.	Evanston Beach sand; Laboratory tests

Reference	D_{50} (mm)	C_u	D_r %	$^1\sigma_v'$ (kPa)	T (°C)	Densification	Measured Time Period	Improvement with Time	Notes
Schmertmann et al. (1986)	NA	NA	20-60	0-100	20	Dynamic Compaction	80 days	As much as 240% increase in q_c in 80 days. No sensitivity.	Florida coastline. Very loose to dense fine sand with trace silt and silty clay seams.
Jefferies et al. (1988)	0.30-0.40	NA	NA	0-200	0	Hydraulic Fill	257 days	No Aging Effects	Erksak fill; < 8% silt
Massarch and Heppel (1991)	NA	NA	NA	0-200	NA	MRC Vibratory Probe	~1 year	q_c increased 50% after 1 year	Considerable scatter in the time dependent data; Marine environment
Charlie et al. (1992)	2.1-2.3	4.17-5.75	70-85	30-90	10	Blasting	5.5 years	Tip resistance increased 18% after 18 weeks; increased 211% after 5.5 years; sleeve friction decreased 39% after 18 weeks (42% after 5.5 years); Initial sensitivity	80% quartz; 10% igneous and metamorphic; 5% feldspar
Gohl et al. (1992)	NA	NA	loose	NA	NA	Blasting	450 days	After 450 days, some increases in q_c was measured, but it was not consistent throughout site	Kelowna, British Columbia
AGRA (1995)			40	0-200	0	Blasting	30 days	200-300% increase in q_c after 12 days; no further increase after 30 days	Sept. Iles, Quebec
Joshi et al. (1995)		2.39	87-95	100	20^2	-	2 years	90% increase in penetration resistance in 1 year for sand submerged in sea water; 80% increase for submerged in distilled water; 30% increase for air dried	River sand Laboratory tests
Joshi et al. (1995)		2.39	87-95	100	20^2	-	2 years	90% increase in penetration resistance in 1 year for sand submerged in sea water; 80% increase for submerged in distilled water; 30% increase for air dried	Beaufort sand Laboratory tests

Notes: 1. For determining stress ranges for field cases, a buoyant unit weight of 10 kN/m^3 was used.

2. Assumed to be 20 °C because tests were performed in a laboratory.

NA = Not available

Table 2.11 Main points of examples of aging effects in sands.

Small Strain Shear Modulus

REFERENCE	MAIN CONCLUSIONS
Afifi and Woods (1971)	As particle size decreases, N_G increases.
Human (1992)	Stress level has no effect on V_α. As relative density decreases, V_α increases. As stress anisotropy increases, V_α decreases. No increase in V_α observed for saturated specimens.
Jamiolkowski (1996)	N_G higher for carbonatic sands than for silica sands.

Conductivity

Brandon and Mitchell (1989) Human (1992)	Thermal resistivity decreased with time and electrical conductivity increased with time for Crystal silica sand. Clay fraction present makes interpretation of effects difficult.

Liquefaction Resistance

Seed (1979)	Liquefaction resistance increased 25% in 100 days in laboratory specimens.
Ishihara (1985) Arango and Migues(1996)	Liquefaction of undisturbed specimens greater than reconstituted specimens.

Stiffness and Shear Strength

Denisov and Reltov (1961)	Sand seemed to "stick" to quartz plate. Difficult to draw conclusions.
Daramola (1980)	50% increase in modulus per log cycle of time. Slight increase in dilatancy with time.
Schmertmann (1991)	Quasi-preconsolidation pressure in sand. Non-standard loading conditions were used.
Human (1992)	No significant increase in modulus or strength with time.
Pender et al. (1992)	Periods of rest caused a repeatable increase in modulus.
Martin et al. (1996)	Biological activity can increase the strength and decrease the hydraulic conductivity of a silty soil.

Table 2.12 Main points of examples of aging effects involving cone penetration tests.

REFERENCE	MAIN CONCLUSIONS
Mitchell and Solymar (1984)	Increases in q_c in hydraulic fill, as well as after blast densification and vibrocompaction. Sensitivity observed following blasting.
Dowding and Hryciw (1986)	Increases in penetration resistance observed at near-zero effective stress conditions in both hydraulic fill and after blast densification in the laboratory.
Hryciw (1986)	No increase in q_c following blasting in saturated loose sands. Presence of surficial clay layer may have hindered drainage.
Schmertmann et al. (1986)	Increases in q_c increased with the number of drops for dynamic compaction (related to energy input). No sensitivity was observed.
Dumas and Beaton (1988)	Profile of improvement with depth following dynamic compaction suggested that increases in q_c were related to energy input. No sensitivity was observed.
Jefferies et al. (1988) Rogers et al. (1990) Jefferies and Rogers (1993)	No increases in q_c for hydraulic fill in sea water at 0^oC. Increases in q_c were observed after blast densification in the same sand at the same temperature. No sensitivity was observed.
Thomann (1990)	Blast densification in a medium dense sand. q_c decreased and never reached pre-blast values.
Massarch and Heppel (1991)	After vibrocompaction, some increases in q_c were observed. However, a lot of scatter was reported.
Human (1992)	Following an earthquake, some increases in q_c were observed. However, they were discounted because of large variability in q_c at the site.
Charlie et al. (1992)	Following blast densification in dense sand, q_c decreased and took 5.5 years to reach pre-blast values.
Charlie et al. (1992) Jefferies et al. (1993)	Suggested that increases in q_c can be related to temperature. However, a discussion showed that temperature did not have a big influence on the observed increases in q_c.
Gohl et al. (1994)	Following blast densification, scattered increases in q_c were observed throughout the site. No mention of sensitivity.
AGRA (1995) Ground Engineering (1995)	Following blast densification, some sensitivity was observed. Significant increase in q_c observed after 12 days. Temperature was $\sim 0^o$ C.
Joshi et al. (1995)	Increases in penetration resistance in the laboratory for both dry and saturated conditions. Micrograph evidence of precipitation.
Ng et al. (1996)	Following vibrocompaction, increases in q_c observed with no sensitivity.

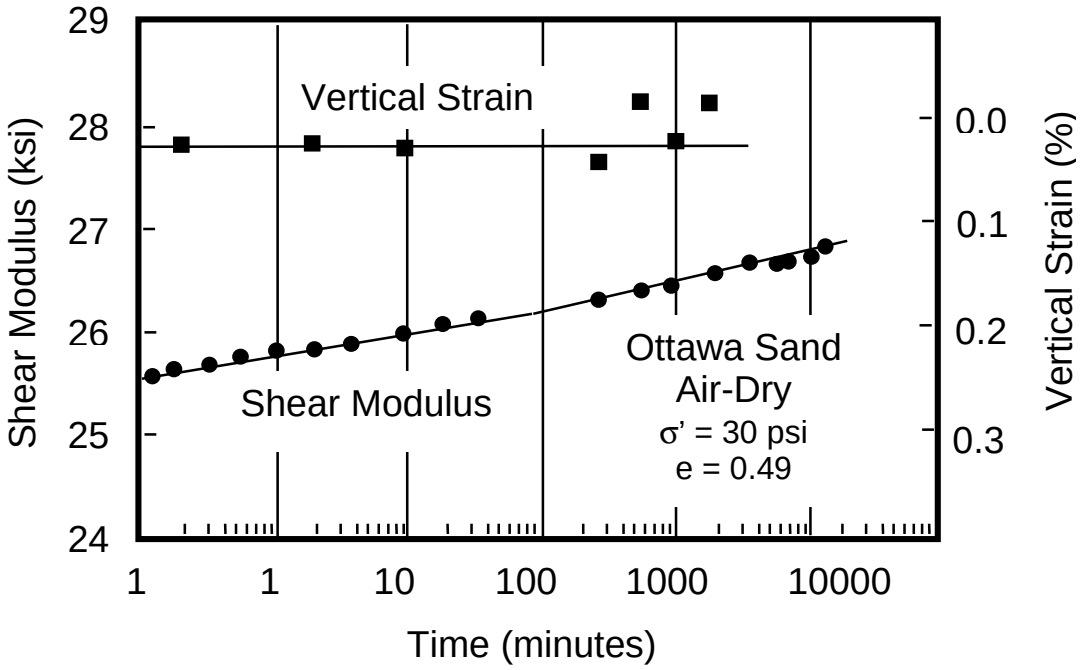

Figure 2.1 Increase in shear modulus with time (Afifi and Woods 1971).

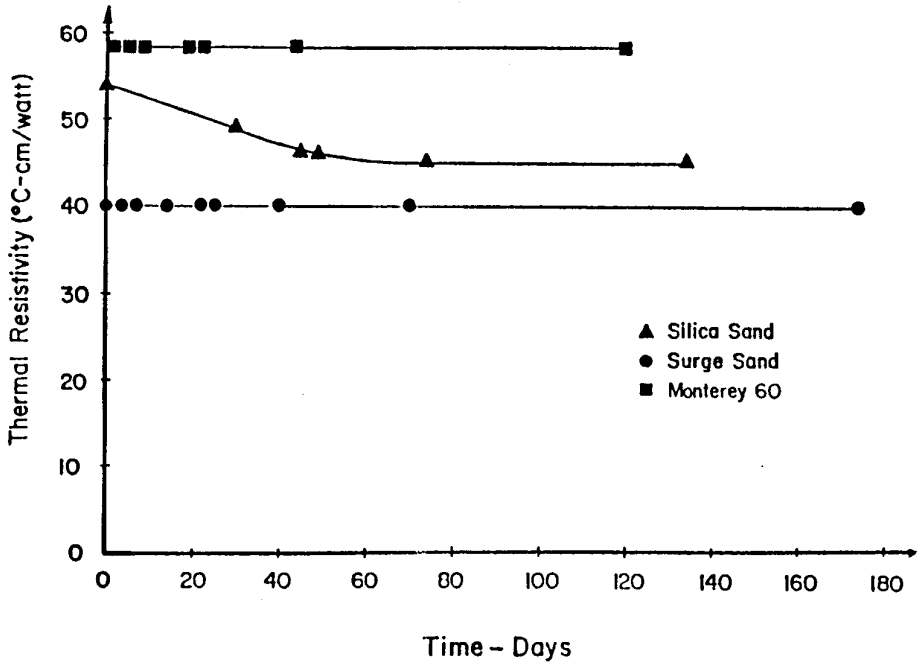

Figure 2.2 Thermal resistivity of three sands with time (Brandon and Mitchell 1989).

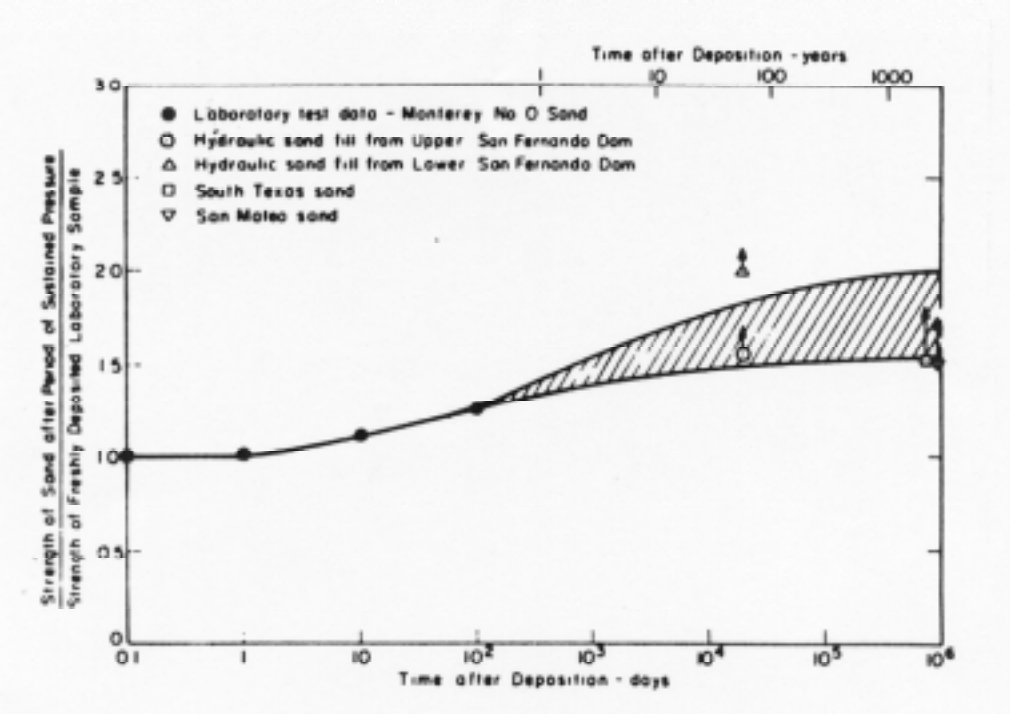

Figure 2.3 Increased Resistance to Liquefaction with Time (Seed 1979).

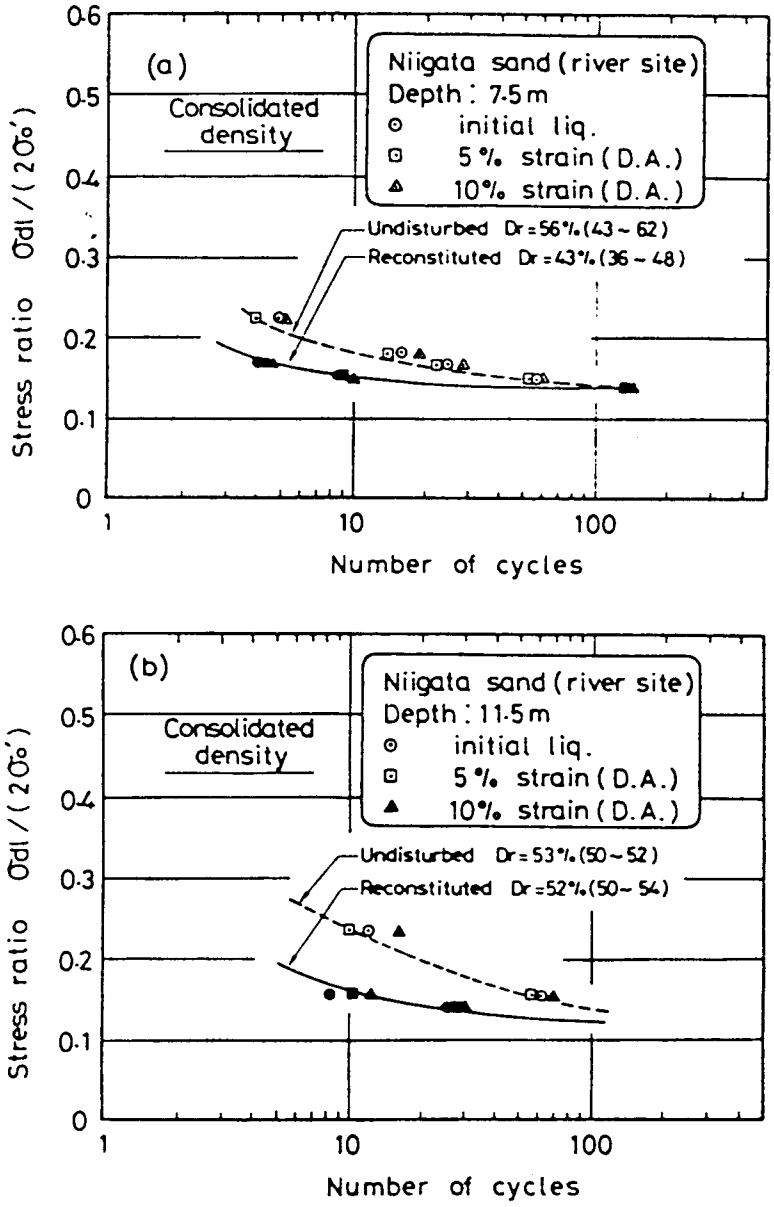

Figure 2.4 Comparison of cyclic strength between undisturbed and reconstituted samples of Niigata sand (Ishihara 1985).

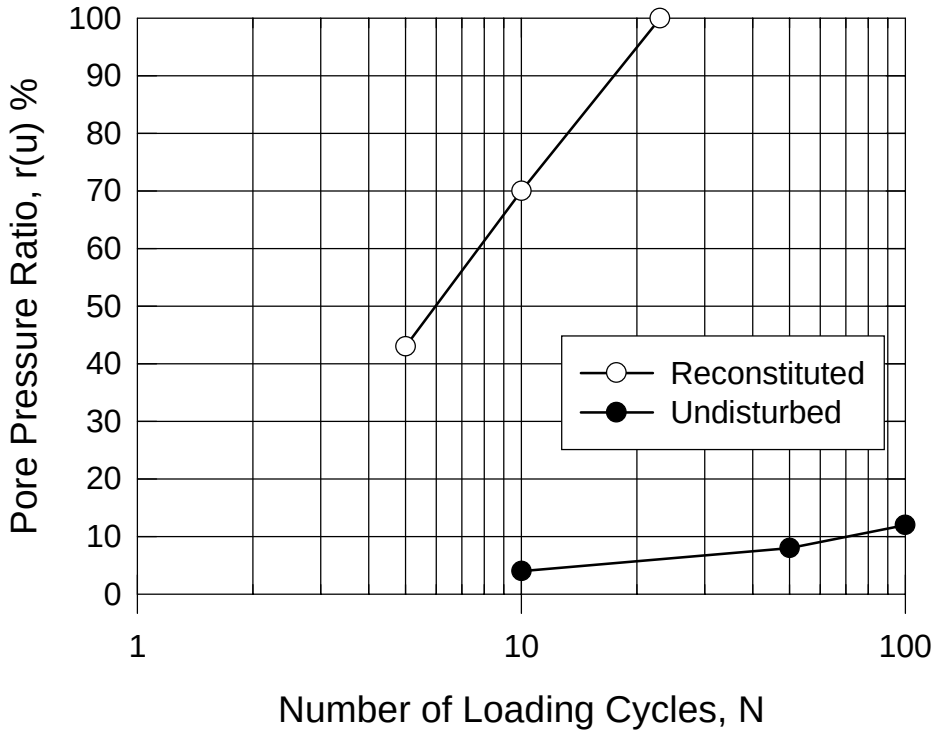

Figure 2.5 Comparison of pore pressure generation in cyclic tests for undisturbed and reconstituted Tapo Canyon sands (Arango and Migues 1996).

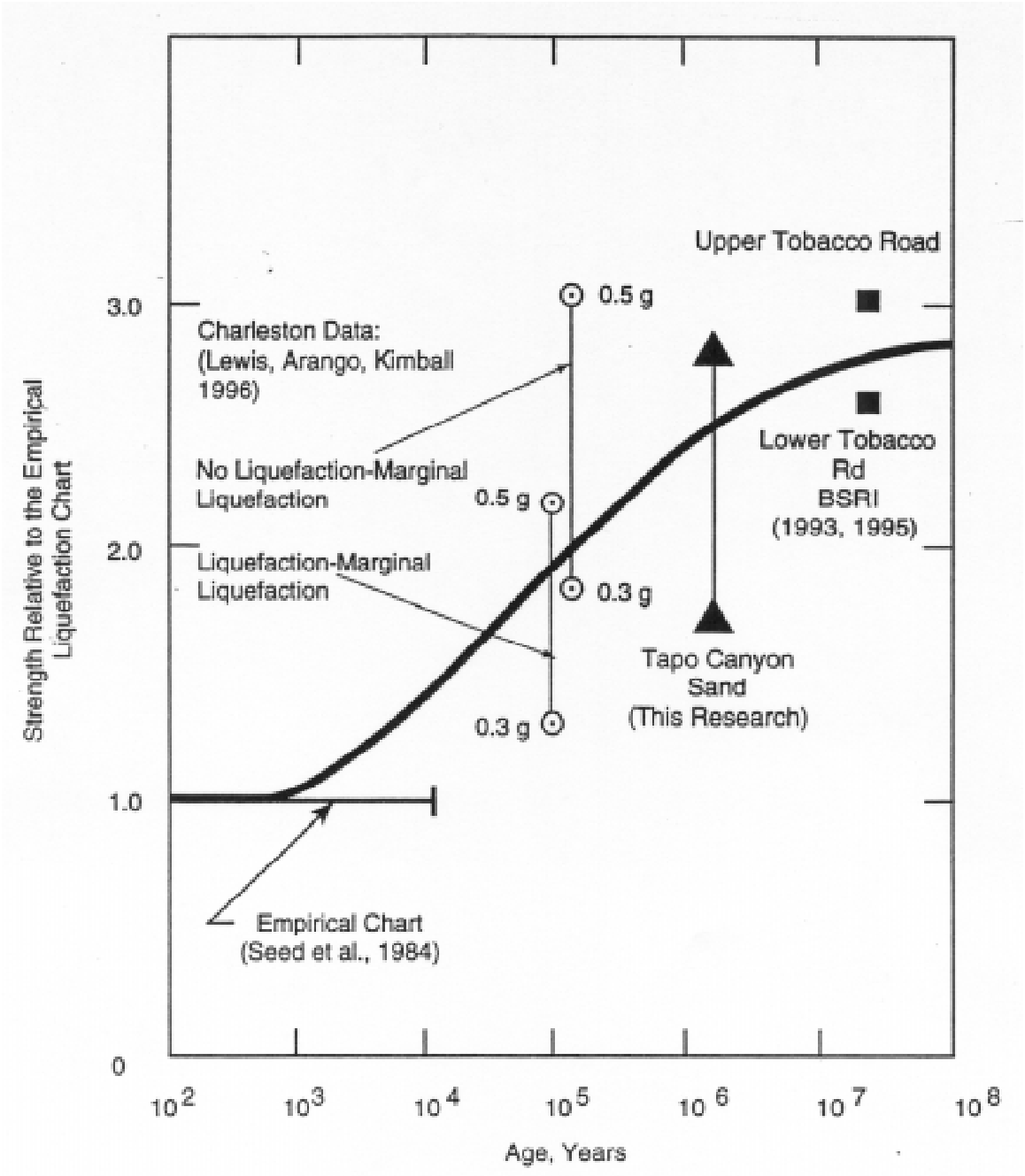

Figure 2.6 Field cyclic strengths of aged sand deposits relative to the strength of Holocene (< 10,000 years) sands (Arango and Migues 1996).

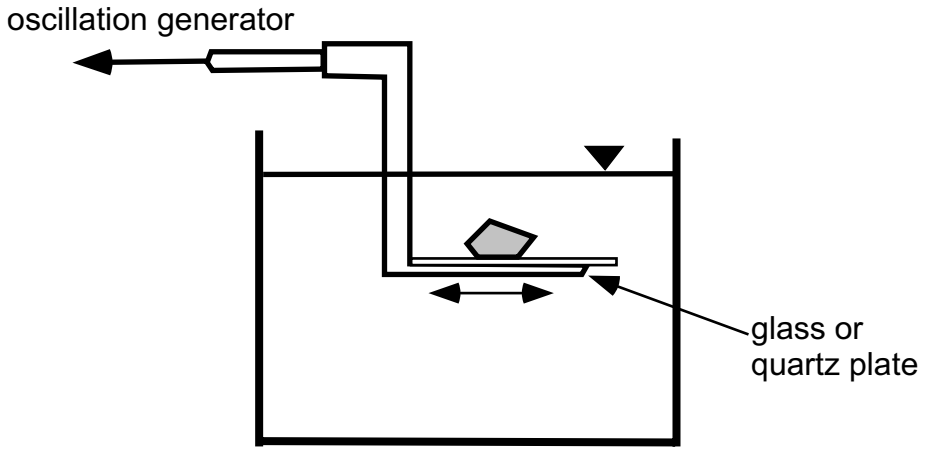

Figure 2.7 Schematic of the vibrating plate experiment (Denisov and Reltov 1961).

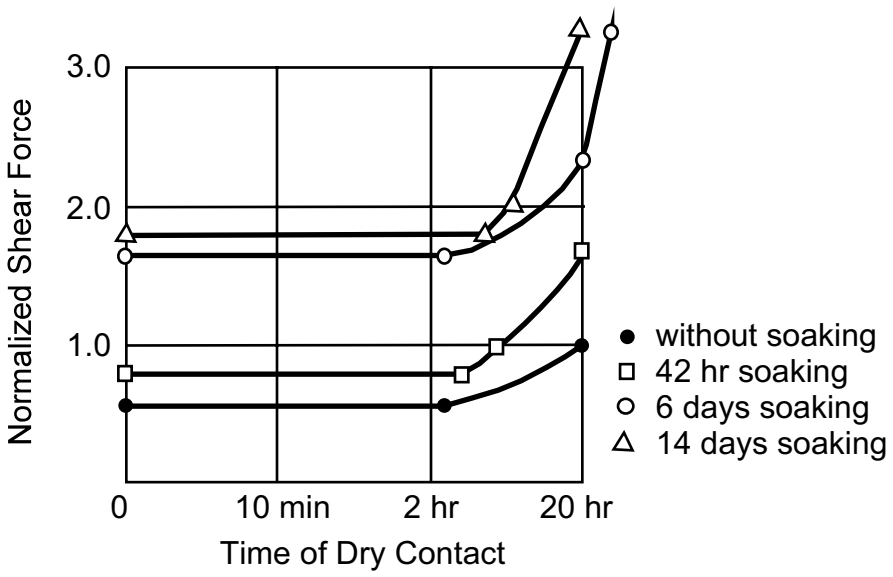

Figure 2.8 Results from the vibrating test experiment (Denisov and Reltov 1961).

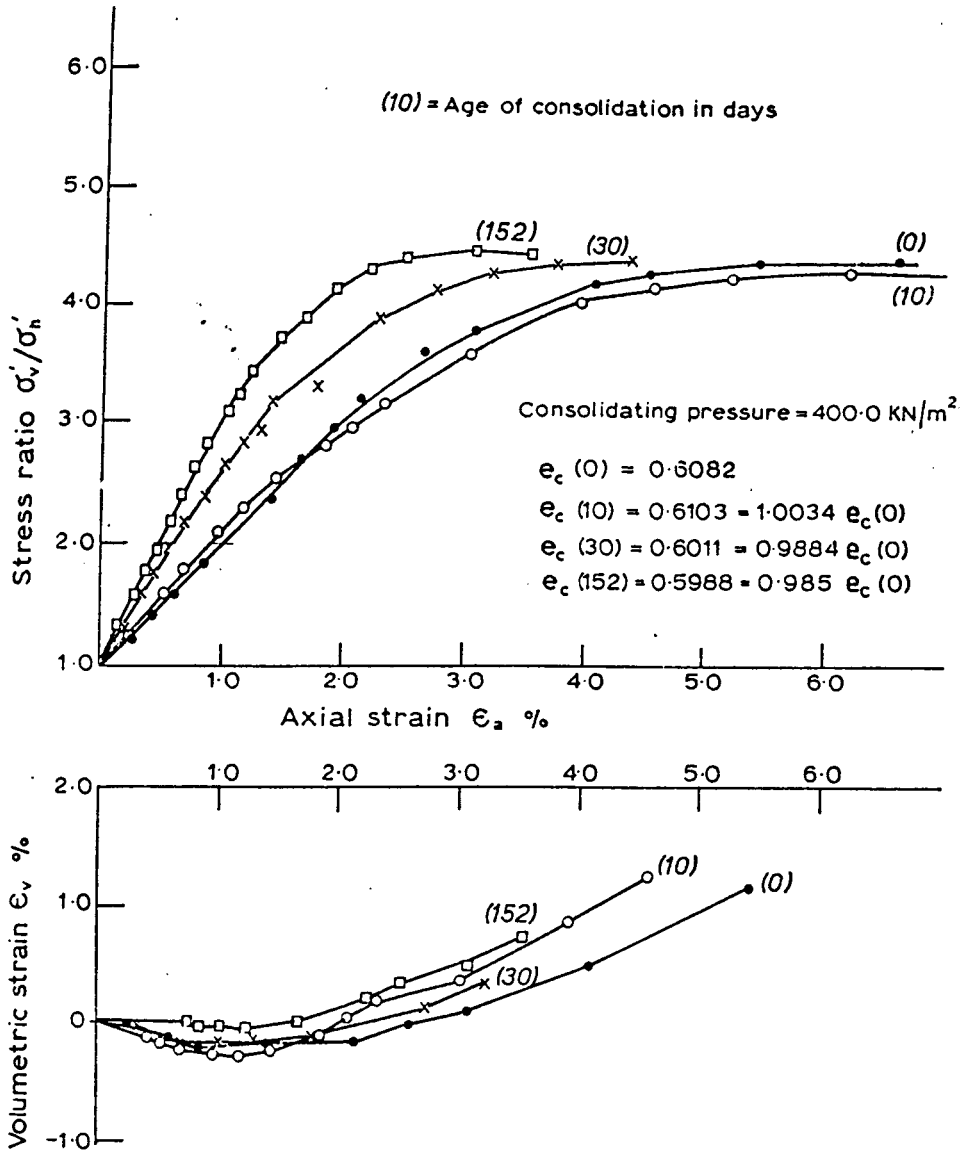

Figure 2.9 Results of triaxial tests on aged samples of Ham River sand (Daramola 1980).

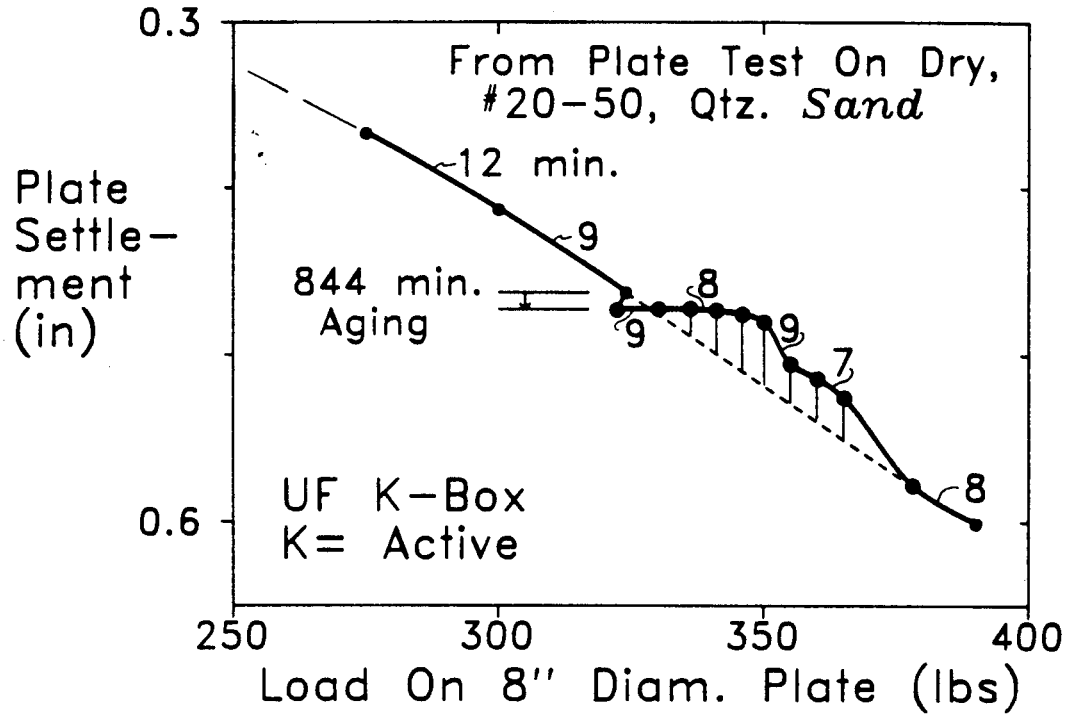

Figure 2.10 Example of quasi-preconsolidation pressure in sand (Schmertmann 1991).

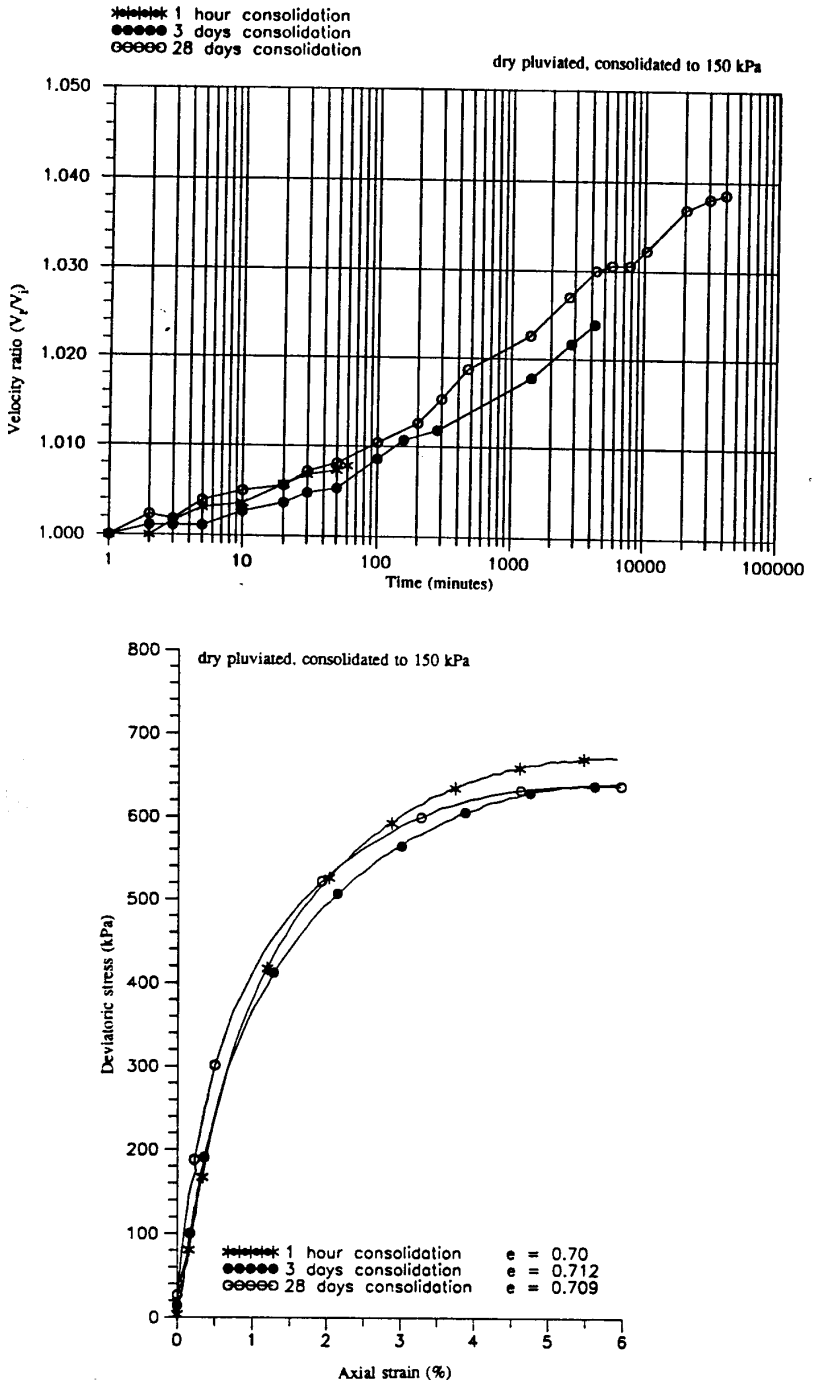

Figure 2.11 Results of three triaxial tests showing (a.) increase in shear wave velocity with time, and (b.) stress – strain relationships (Human 1992).

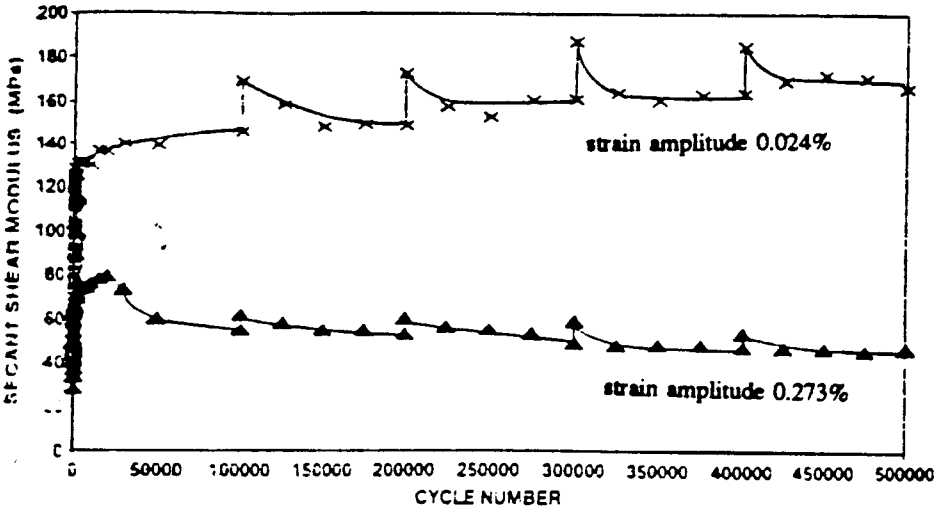

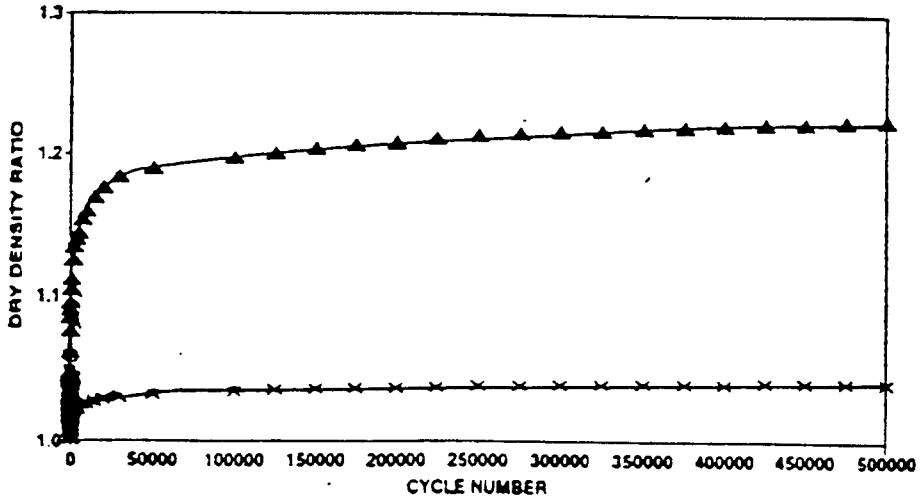

Figure 2.12 Aging effects in simple shear showing (a) an increase in modulus after periods of rest, and (b) changes in density. (Pender et al. 1992).

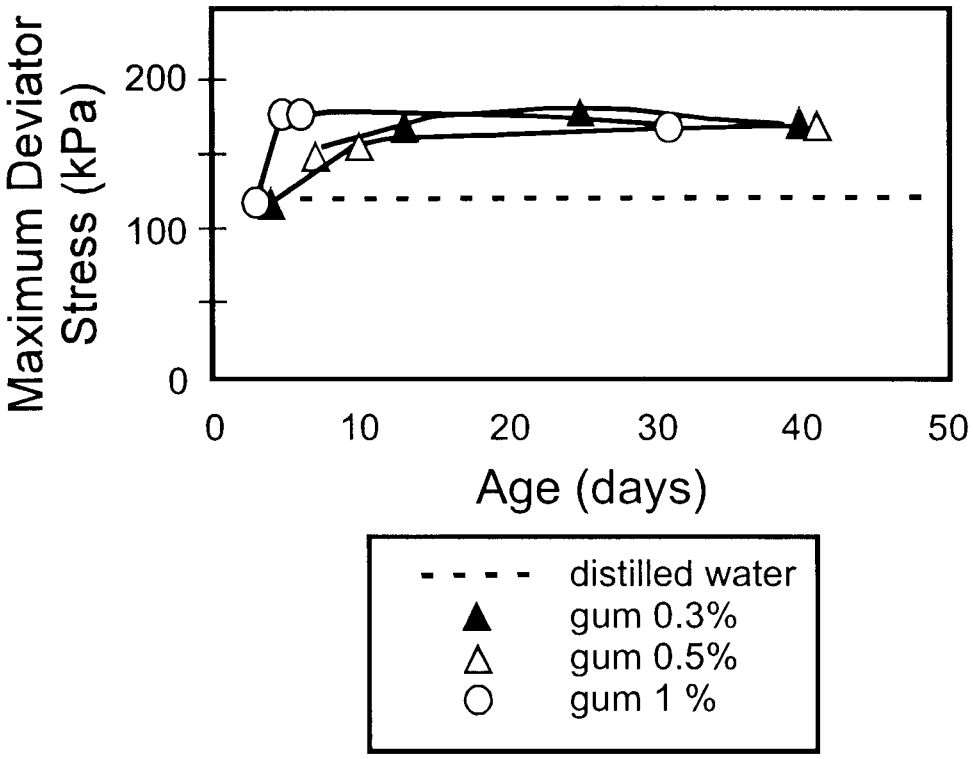

Figure 2.13 Effect of Xanthan gum on the strength of a silt (Martin et al. 1996).

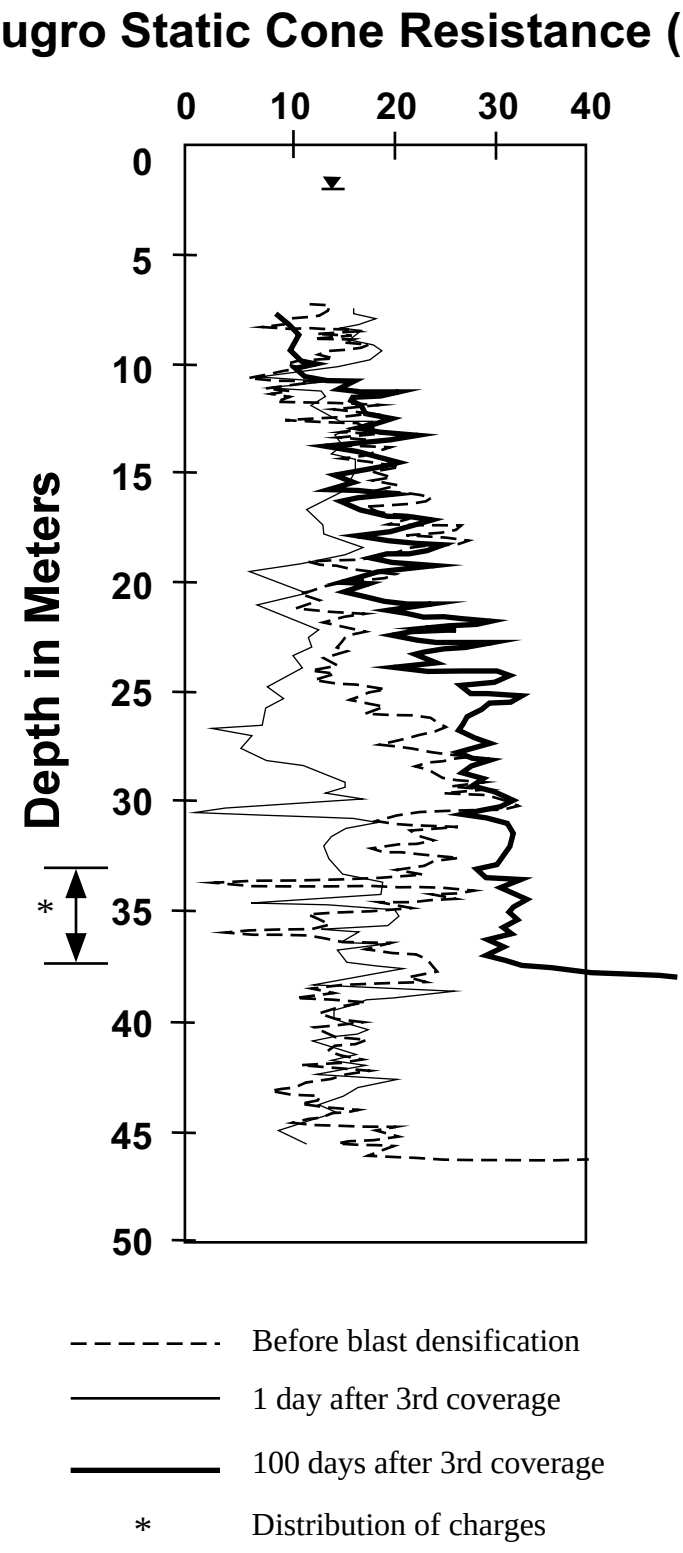

Figure 2.14 Effect of aging after blast densification at Jebba Dam (after Solymar 1984).

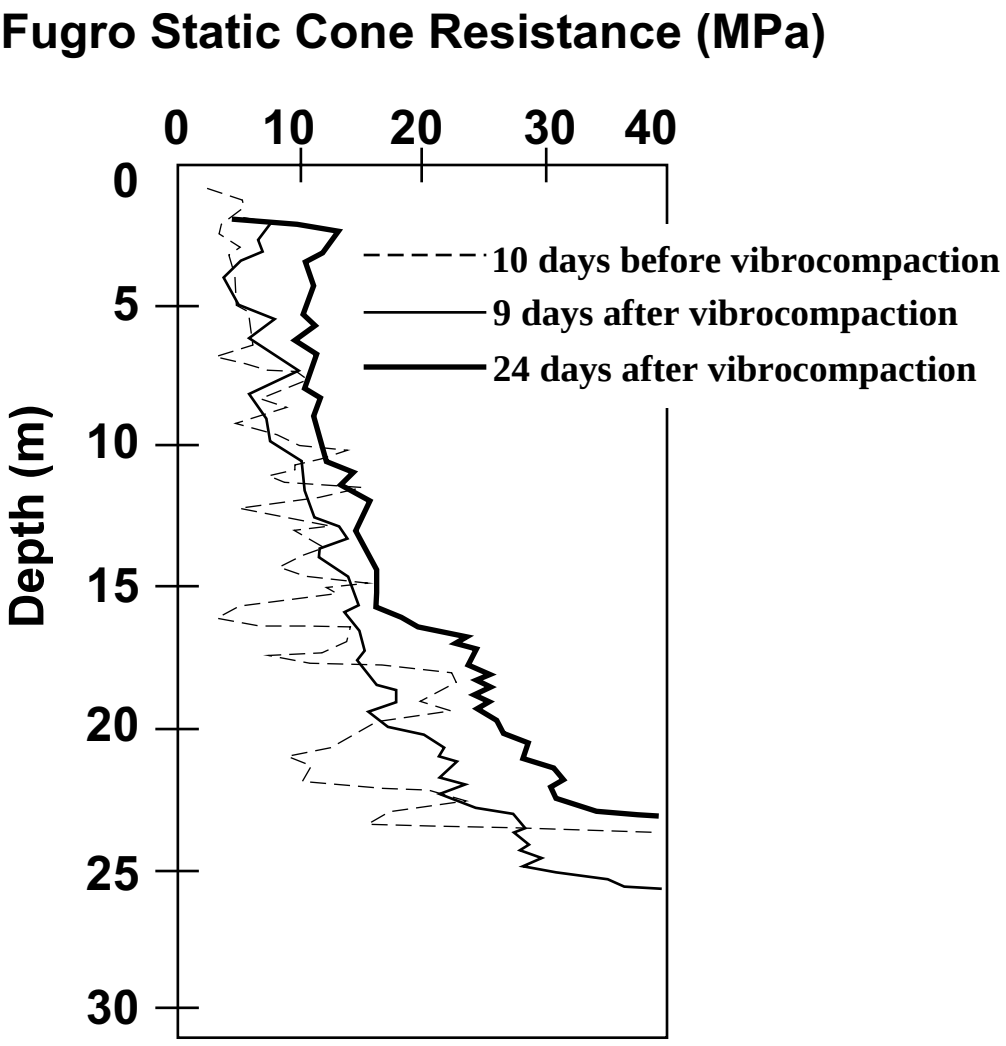

Figure 2.15 Effect of aging after vibrocompaction at Jebba Dam (after Mitchell and Solymar 1984).

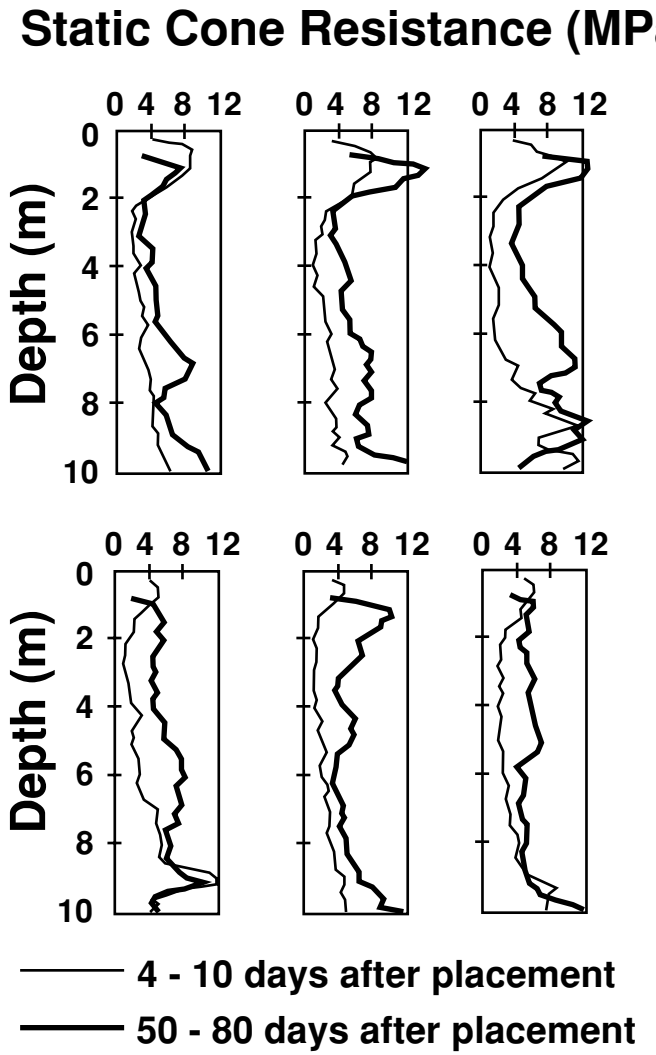

Figure 2.16 Effect of Aging on a hydraulic fill at Jebba Dam (after Mitchell and Solymar 1984).

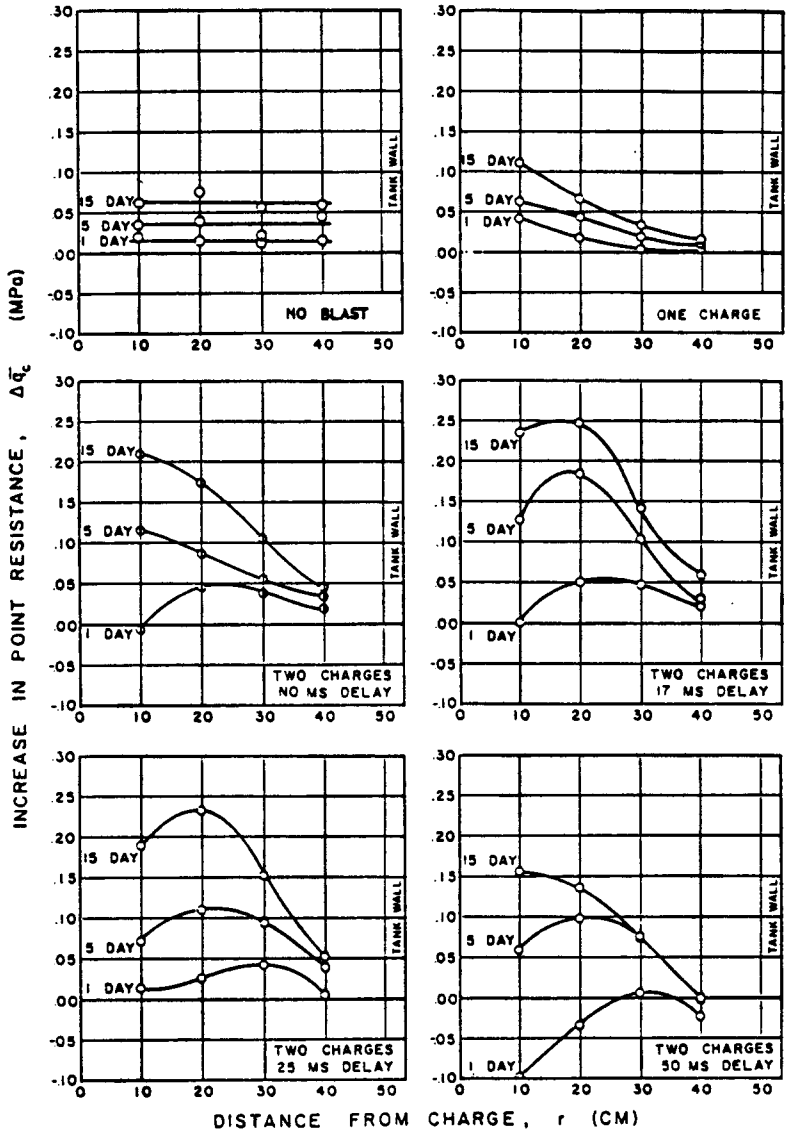

Figure 2.17 Results of aging effects on a laboratory blasting experiment (Dowding and Hryciw 1986).

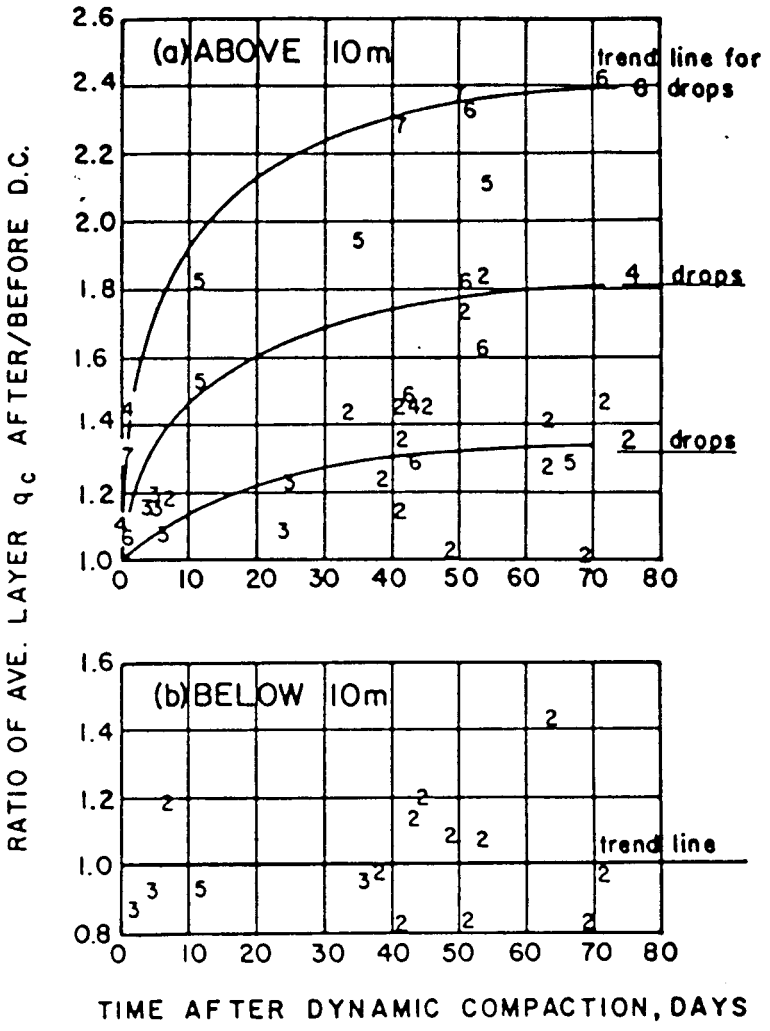

Figure 2.18 Aging effects after dynamic compaction at power park site (Schmertmann et al. 1986).

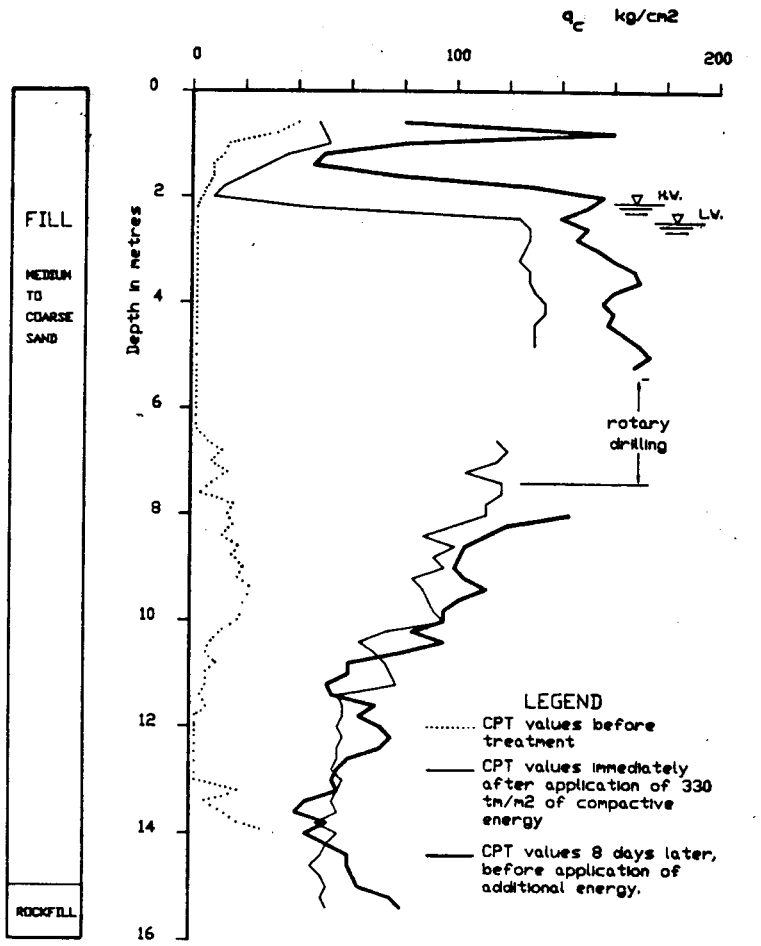

Figure 2.19 Aging effects after dynamic compaction at Pointe Noire deep sea harbor (Dumas and Beaton 1988).

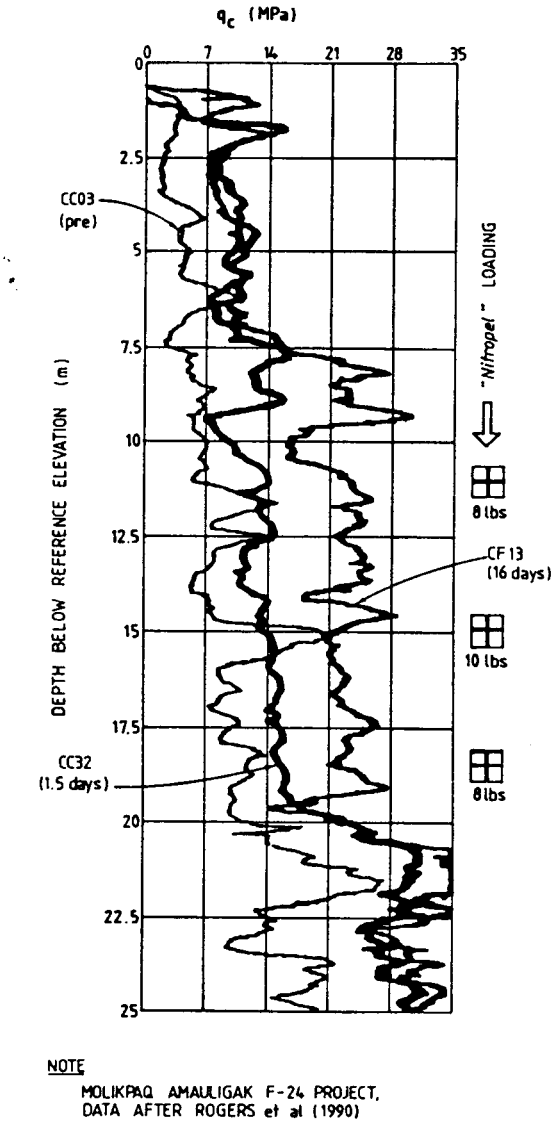

Figure 2.20 Aging effects after blast densification at Moliqpak Amauligak F-24 (Jefferies and Rogers 1993).

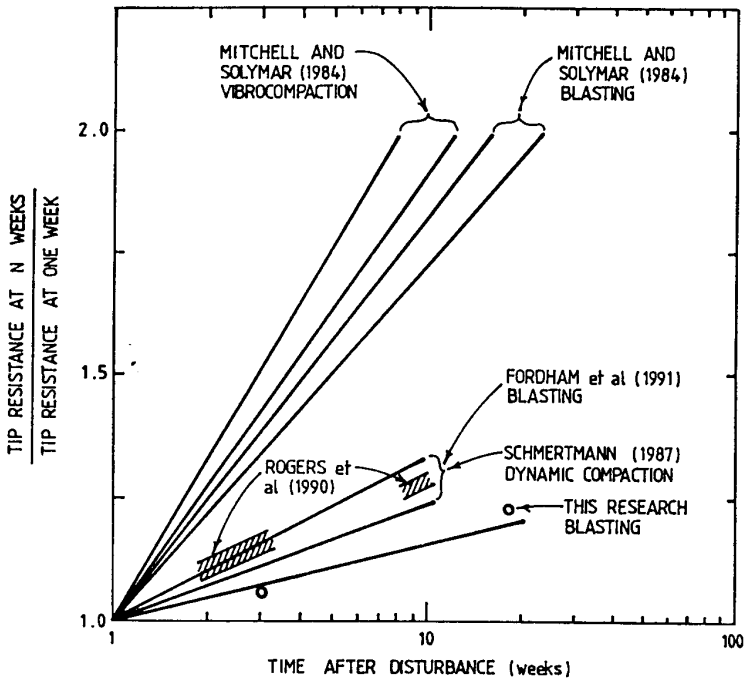

Figure 2.21 Normalized penetration resistance vs. time (Jefferies and Rogers 1993).

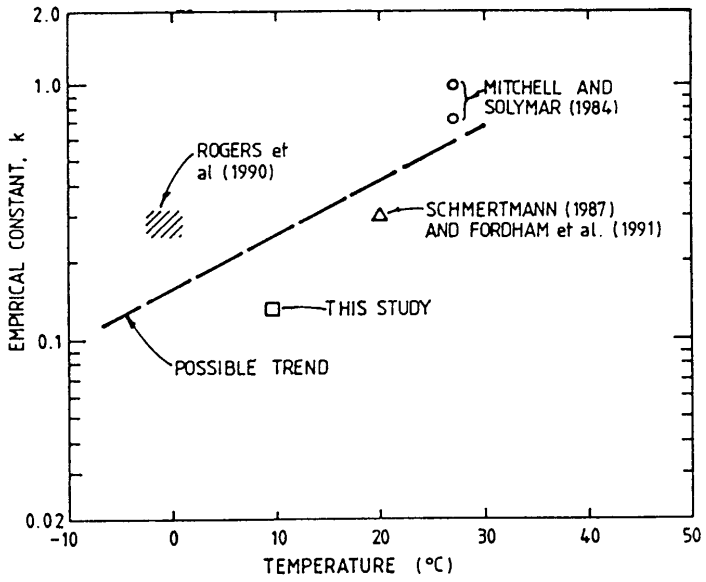

Figure 2.22 Rate of increase in penetration resistance as a function of temperature (Jefferies and Rogers 1993).

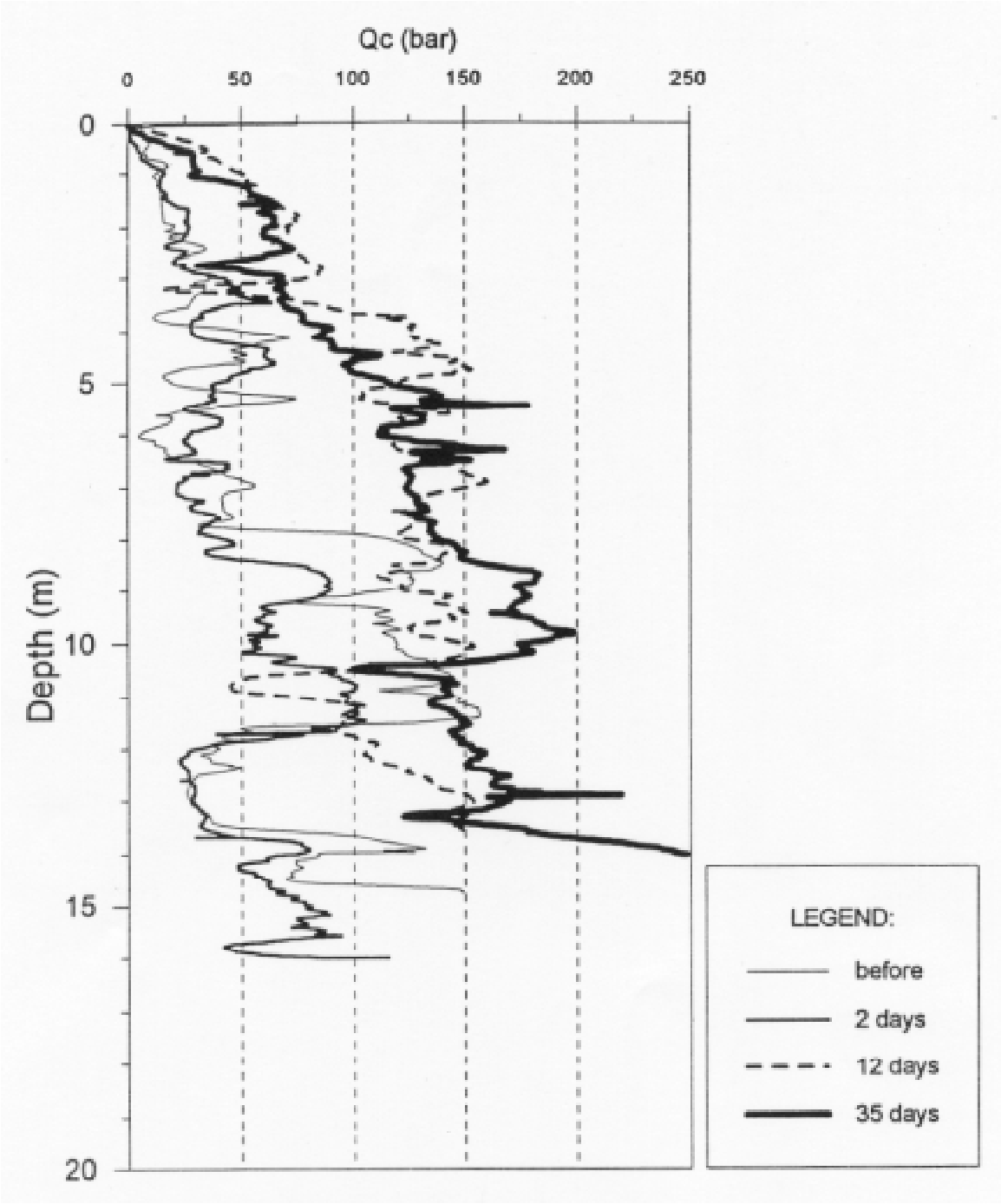

Figure 2.23 Aging effects after blasting at SM-3 Site in Quebec (AGRA 1995).

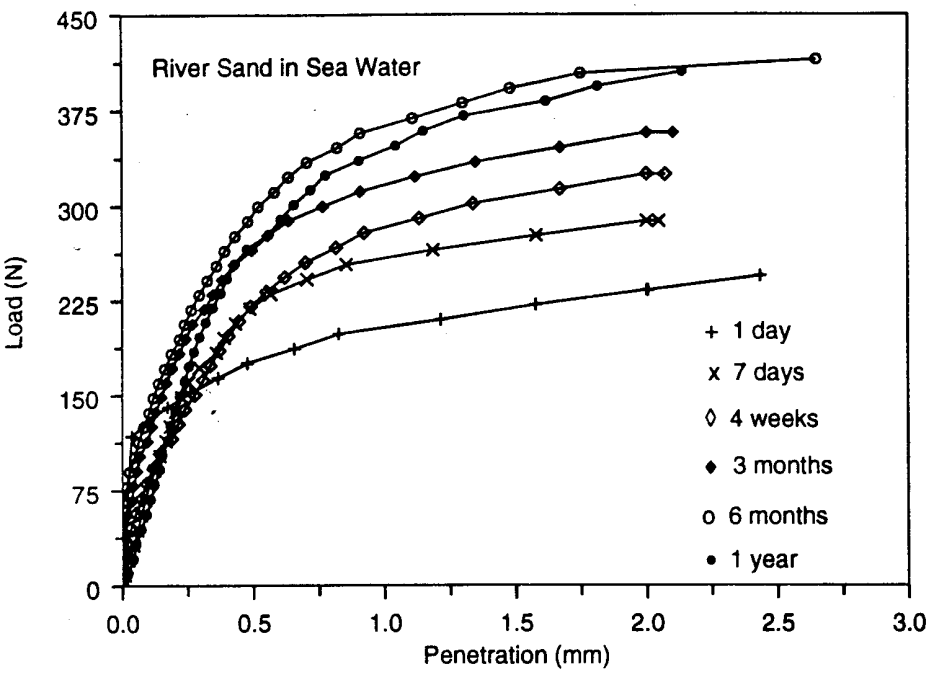

Figure 2.24 Load displacement curves for penetration tests in the laboratory (Joshi et al. 1995).

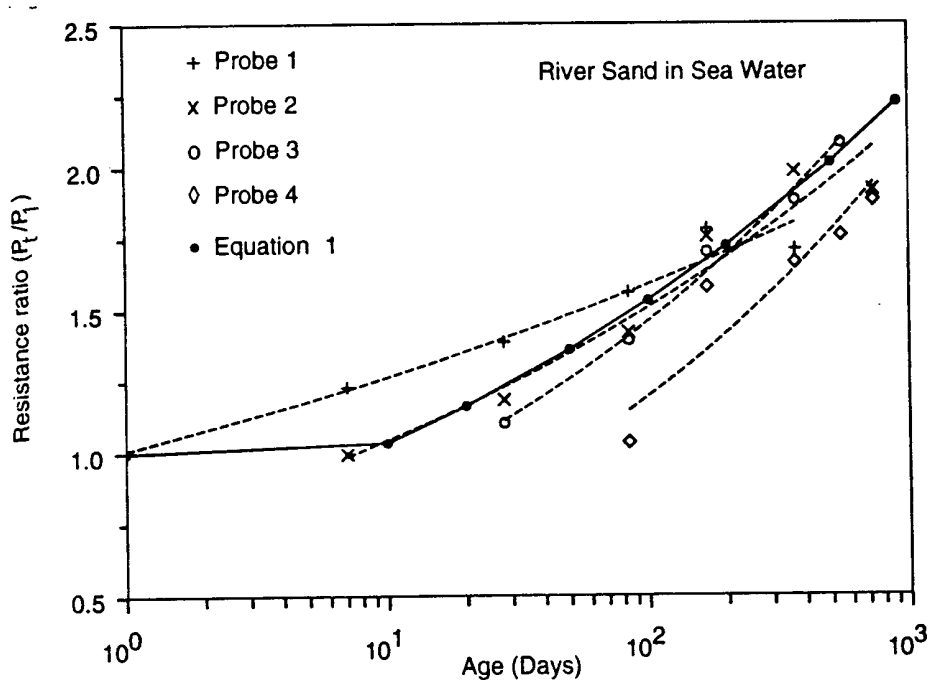

Figure 2.25 Increase in penetration resistance with time for laboratory specimens (Joshi et al. 1995).

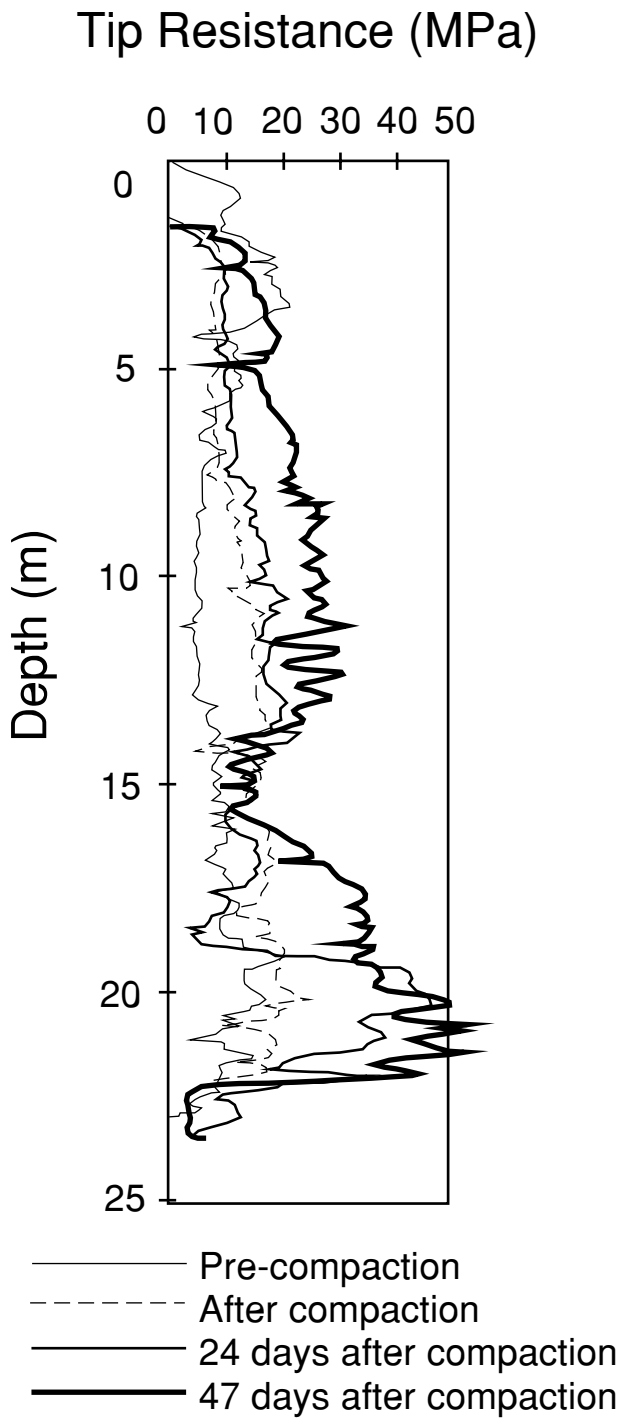

Figure 2.26 Effect of aging after vibrocompaction at Chek Lap Kok airport (after Ng et al. 1996).